Artificially stimulating retrotransposon activity increases mortality and accelerates a subset of aging phenotypes in *Drosophila*

Joyce Rigal[1], Ane Martin Anduaga[1], Elena Bitman[1], Emma Rivellese[1], Sebastian Kadener[1], Michael T. Marr II[1, #,+]

[1] Biology Department, Brandeis University, Waltham, MA, 02454, USA.

[#] To whom correspondence should be addressed

Michael T. Marr II mmarr@brandeis.edu

+ Lead Contact

ABSTRACT:

Transposable elements (TE) are mobile sequences of DNA that can become transcriptionally active as an animal ages. Whether TE activity is simply a byproduct of heterochromatin breakdown or can contribute towards the aging process is not known. Here we place the TE *gypsy* under the control of the UAS GAL4 system to model TE activation during aging. We find that increased TE activity shortens the lifespan of male *D. melanogaster.* The effect is only apparent in middle aged animals. The increase in mortality is not seen in young animals. An intact reverse transcriptase is necessary for the decrease in lifespan implicating a DNA mediated process in the effect. The decline in lifespan in the active *gypsy* flies is accompanied by the acceleration of a subset of aging phenotypes. TE activity increases sensitivity to oxidative stress and promotes a decline in circadian rhythmicity. The overexpression of the Forkhead-box O family (FOXO) stress response transcription factor can partially rescue the detrimental effects of increased TE activity on lifespan. Our results provide evidence that active TEs can behave as effectors in the aging process and suggest a potential novel role for dFOXO in its promotion of longevity in *D. melanogaster*.

INTRODUCTION

Aging leads to a progressive loss of physiological integrity that culminates in a decline of function and an increased risk of death (López-Otín et al., 2013). It is a universal process that involves the multifactorial interaction of diverse mechanisms that are not yet fully elucidated. Transposable elements (TE) are among the many factors that have been proposed to be involved in aging (Morley, 1995; Wood & Helfand, 2013). TE are present in every eukaryotic genome sequenced to date (García Guerreiro, 2012; Huang et al., 2012). They are sequences of DNA that can move from one place to another (McCLINTOCK, 1950), either by reverse transcription and insertion into the genome (Class 1: Retrotransposons), or through direct excision and movement of the element (Class 2: DNA TE) (McCullers & Steiniger, 2017).

Multiple studies (Gorbunova et al., 2021) report that TE mRNA levels increase in the aging somatic tissue of flies (Giordani et al., 2021; Li et al., 2013; Wood et al., 2016), termites (Elsner et al., 2018), mice (De Cecco, Criscione, Peterson, et al., 2013), rats (Mumford et al., 2019) and humans (LaRocca et al., 2020). A direct correlation to an increase in genomic copy number has been difficult to determine (Treiber & Waddell, 2017; Yang et al., 2022). Nonetheless, clear evidence for an increase of TE somatic insertions with age has been obtained using reporter systems. Two reporter systems for insertions of the long-terminal-repeat (LTR) retrotransposon *gypsy* demonstrate that *gypsy* insertions increase during aging in the *D. melanogaster* brain and fat body (Y.-H. Chang et al., 2019; Li et al., 2013; Wood et al., 2016).

TE movement in somatic tissue has been proposed to be a driver of genomic instability (Ivics & Izsvák, 2010) and potentially aging (Morley, 1995; Wood & Helfand, 2013; Woodruff & Nikitin, 1995). Additionally, TE activity has been reported to cause disease in humans (Hancks et al., 2012). Current research reports that long-interspersed-element-1 (*L1)* activity itself, without an increase in insertions, can trigger an inflammation response that contributes to aging related phenotypes in human senescent cells (Cecco et al., 2019). In aged mice, the use of reverse transcriptase inhibitors can downregulate this age associated inflammation (Cecco et al., 2019) implicating retrotransposons. The shortened lifespan of a Dicer-2 (*dcr-2)* mutant fly strain, which has an increase of TE expression, can also be extended by the use of reverse transcriptase inhibitors (Wood et al., 2016). In summary, current evidence suggests a role for TE activity in aging.

However, whether the role of TE activity is as effector or bystander of the aging process is an open question. As an animal ages, heterochromatin repressive marks decrease and resident silent genes can become expressed (Jiang et al., 2013). TE sequences are enriched in silent heterochromatin and thus become expressed (De Cecco, Criscione, Peckham, et al., 2013). This raises the question of whether TE expression is simply a byproduct of age-related heterochromatin breakdown or if TE themselves can contribute to the aging process. To date, this has not been directly assayed.

To combat the effects of TE activity, cells have evolved small RNA pathways to maintain silencing of TE. The PIWI pathway dominates in the germline while the

somatic tissue of *Drosophila* is thought to mainly rely on the siRNA pathway (Hyun, 2017). This pathway is based on Dicer-2 cleaving double stranded (ds) RNA precursors, generally viral genomes or TE dsRNA, into small RNAs that are loaded into Ago2 guiding the RNA Induced Silencing Complex (RISC) to cleave its targets (Hyun, 2017). In *D. melanogaster*, endogenous siRNAs in RISC mapping to TE loci have been reported (Czech et al., 2008; Ghildiyal et al., 2008; Kawamura et al., 2008). The mutation, knockdown, or depletion of genes involved in the siRNA pathway such as *Dcr-2* (Lee et al., 2004) and *AGO2* (Okamura et al., 2004) leads to increased expression of TE in somatic cells and a shortened lifespan (Kawamura et al., 2008; Czech et al., 2008; Chung et al., 2008; Lim et al., 2011; Li et al., 2013; Wood et al., 2016; Chen et al., 2016). On the other hand, the overexpression of *Dcr-2* (Wood et al., 2016) and *AGO2* (Yang et al., 2022) in adult fly somatic tissue can lower TE expression and extend lifespan. Taken together, these results suggest TE activity can influence lifespan. The effect of TE activity on lifespan has not been directly determined.

The Forkhead-box O family (FOXO) is an evolutionarily conserved transcription factor capable of enhancing longevity by enabling the cell to respond to diverse stress signals (Calnan & Brunet, 2008). The longevity effects of FOXO have been reported in worms, flies, and mice (Martins et al., 2016). FOXO activity can enable transcriptional responses to provide protective effects against cellular stress: oxidative stress, heat shock, virus infection, and defects in protein homeostasis among many others (Donovan & Marr, 2016; Martins et al., 2016; Spellberg & Marr, 2015). Whether TE activity is a condition that FOXO activity might protect against is unknown.

In this study we have set up a system to directly assay if TE can become active contributors of the aging process. For this, we placed the retrotransposon *gypsy* (Bayev et al., 1984), which will be used as a candidate to model TE activity during aging, under the control of the UAS GAL4 system (Brand & Perrimon, 1993). The retrotransposon *gypsy* is a TE that has been clearly shown to become active in aged *D. melanogaster* somatic tissue under natural conditions (Li et al., 2013; Wood et al., 2016). In our system, we find that active TE expression significantly increases the mortality in middle aged flies and that an intact reverse transcriptase is necessary for this effect. The increase in mortality is accompanied by acceleration of a subset of aging-related phenotypes. We find that the FOXO homologue in *Drosophila* (dFOXO) can counteract and partially rescue the decrease in lifespan generated by an active TE, suggesting a possible novel mechanism through which dFOXO might promote longevity in *D. melanogaster*.

RESULTS

To determine dFOXO's possible involvement in TE regulation we sequenced the RNA from whole animals of 5-6 days (d) and 30-31d old w^{DAH} (wt) and dFOXO deletion ($w^{DAH\ \Delta 94}$) males (Slack et al., 2011). These lines have been extensively backcrossed, making them isogenic other than for the dFOXO deletion (Slack et al., 2011). In these conditions, the wt animals display significant increased expression of two TEs (*1731* and *Doc4*) and decreased expression of two additional TEs (*Stalker2* and *G6*) with age (Fig. 1a, 1b and 1-S1). By contrast, in the dFOXO deletion animals, 18 TEs exhibited a significant increase in expression with age (Fig. 1c, 1d and 1-S2) while no TE

125 expression decreased with age indicating the overall TE load is greater in the aged
126 dFOXO deletion flies.

127 The vast majority of TE expression levels in both strains fall within the observed
128 range of average gene expression (Fig. 1a and Fig. 1d). Total TE expression undergoes
129 a small change overall in both genotypes. Expression increased only 1.2-fold with age
130 (Fig. 1-Table S1) in wt flies and 1.41-fold in dFOXO null flies (Fig. 1-Table S2). Of the
131 two TE that increased with age in wt flies, only *1731* exhibits an increase in dFOXO null
132 flies. Among the two TE that decreased with age in wt, *G6* showed the opposite effect
133 on expression in dFOXO null flies while *Stalker2* showed no change with age in dFOXO
134 null flies. The direct comparison of individual TE expression levels in young wt and
135 dFOXO null flies indicates that despite being backcrossed (Slack et al., 2011) different
136 TE are being expressed in each strain (Fig. 1e). This means that the otherwise isogenic
137 lines have a different transcriptionally active TE landscape. Therefore, beyond the
138 comparison of the number of transcriptionally active TE, a direct comparison between
139 wt and dFOXO null flies to determine the effect of dFOXO on any specific TE
140 expression during aging is challenging.

Figure 1. TE expression increases with age in FOXO null flies.

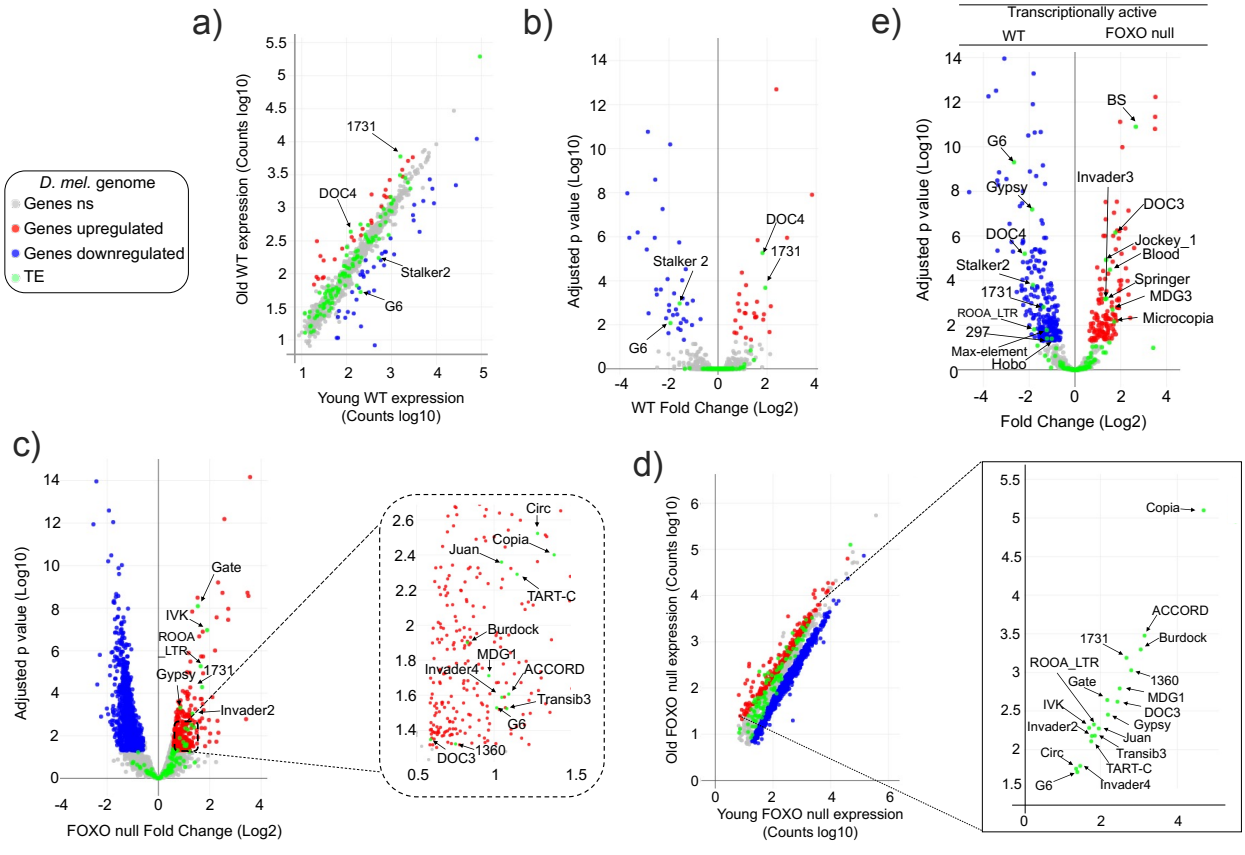

Figure 1. TE expression increases with age in FOXO null flies. Data represents RNAseq from 3 biological replicates (10 male flies per sample). Young – 5 days, Old – 30 days. Legend (grey: fly genes not significant (ns), red: upregulated fly genes, blue: downregulated fly genes, green: TE). Differential expression indicates a 1.5-fold change or higher and an adjusted p value < 0.05, as determined by DEseq2. a-d) Red indicates upregulation with age. Blue denotes downregulation with age. Significantly different TE are identified by name. a-b) Wildtype (WT) control. 4 TE are labelled. c-d) FOXO null. 18 TE are labelled. e) Volcano plot of young WT control and young FOXO null. Red and blue dots indicate gene relative expression in FOXO null compared to WT, respectively. TE are marked by green dots. Adjusted p values for each TE are provided in Figure 1-Table supplement 1 (WT) and Figure 1-Table supplement 2 (FOXO null)

153 Our difficulties to determine the effect of dFOXO on any specific TE highlights the
154 need for a controlled system to test TE expression and regulation during aging. The
155 *gypsy* retrotransposon was selected as a model system to study TE activity and we
156 developed a UAS-*gypsy* system. The structure of the ectopic UAS-*gypsy* system is
157 depicted in Fig. 2a. A direct comparison to the endogenous *gypsy* element can be
158 observed in a simplified overview of three broad stages in the *gypsy* lifecycle (parental
159 element, propagation through transcription and reverse transcription, and new
160 insertion). The presence of the UAS promoter in the ectopic *gypsy* allows the control of
161 *gypsy* expression by mating to a GAL4 expressing strain. In addition, we inserted a
162 unique sequence tag in the 3' LTR of the ectopic *gypsy* to differentiate it from the
163 endogenous copy of *gypsy* (Bayev et al., 1984, p. 4). We inserted the UAS-*gypsy*
164 construct in the VK37 attP site on chromosome 2 using the PhiC31 system (Venken et
165 al., 2006). Using this approach, we found that ectopic *gypsy* expression is significantly
166 induced when the line is crossed to a strain in which gal4 is ubiquitously expressed
167 under the *ubiquitin* promoter (*Ubi>gypsy*) (Fig. 2b).

168 This tag also allows us to take advantage of the strand transfer that occurs
169 during reverse transcription of the retroelement before integrating into a new site in the
170 genome. This process replaces the UAS sequence with a 5' LTR and transfers the
171 sequence tag to the new LTR of the newly integrated *gypsy* element (Weaver, 2008)
172 (Fig. 2a). Using this approach, we found that new insertions are created and can be
173 specifically detected (Fig. 2c) when UAS-*gypsy* is expressed (*Ubi>gypsy* genotype).
174 The junction between the recombinant *gypsy* 5' LTR and the *gypsy* provirus sequence
175 is only formed when a complete insertion is made. Sanger sequencing of the qPCR

176 insertion products demonstrates the specific detection of this junction, indicating that the

177 UAS-*gypsy* element can transpose and is an active TE element (Fig. 2d).

Figure 2. UAS-*gypsy* structure and functional test.

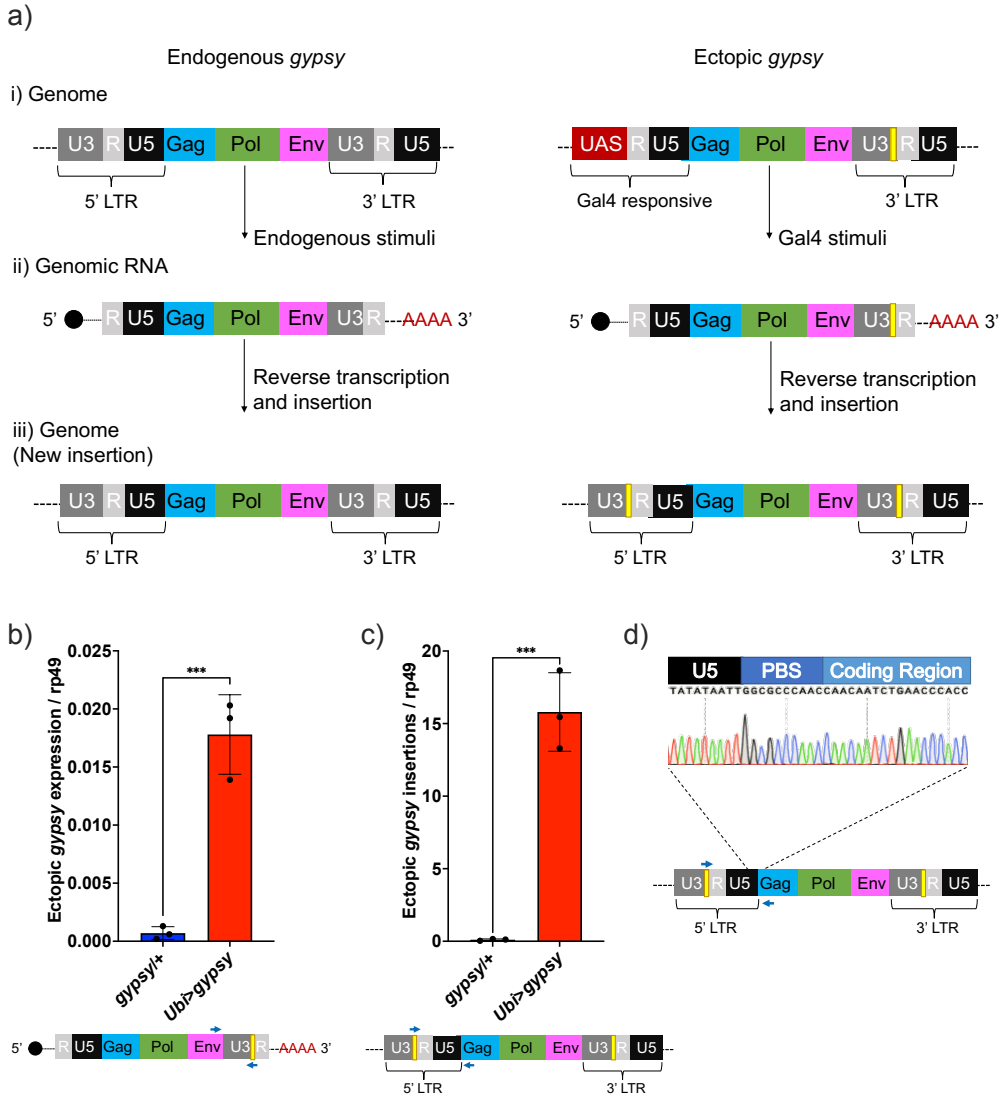

Figure 2. UAS-*gypsy* structure and functional test. a) Simplified overview of 3 stages of the *gypsy* retrotransposon lifecycle, i) parent insertion in the genome, ii) the transcribed RNA (genomic RNA), and iii) the new copy inserted in the genome. The difference between the wildtype *gypsy* and ectopic *gypsy* resides in both its 5' and 3' LTR. The presence of an upstream activating sequence (UAS) in the 5' LTR allows *gypsy* to be transcribed in response to a Gal4 stimuli. In the 3' LTR, the addition of a unique sequence of DNA (denoted by a yellow square) not found in the *D. melanogaster* genome allows quantification and tracking of new insertions by molecular methods. b) RT-qPCR of 5-day old males. 3' end of ectopic *gypsy* transcript is detected. Data are represented as means ± SD (3 biological replicates, each dot is a pool of 5 flies). One-tailed t test, *** p value 0.0005. c) gDNA qPCR of 5-day old males. Ectopic *gypsy* provirus insertion junctions are detected. Data are represented as means ± SD (3 biological replicates, each dot is a pool of 10 flies). One-tailed t test, *** p value 0.0003. d) Sanger sequencing of the newly created ectopic *gypsy* provirus insertion junction in *Ubi>gypsy* flies.

To characterize the spectrum of insertion sites of the UAS-*gypsy* construct we took a targeted sequencing approach. Using a biotinylated primer hybridizing with the unique sequence tag oriented to read out from the newly integrated 5' LTR we created Illumina Next generation sequencing libraries to sequence the genomic junctions (Fig. 3-S1a). Libraries were prepared from three biological replicates of ten 14-day old male flies each. Sequencing reads were sorted using the LTR sequence as a barcode. After removing the LTR sequence, the exact site of insertion was mapped back to the *Drosophila* reference genome. More than 11,000 insertion sites were identified. Sites were identified in all chromosomes with the fraction of insertions roughly correlating with the size of the chromosome (Fig. 3A). Comparing the insertion sites with the genome annotation allowed us to classify the insertion sites. Sixty-six percent of the mapped insertion sites are in transcribed regions (Fig. 3B). Of those sites, the majority are in intronic regions (Fig. 3C). Because the data provides nucleotide resolution, we could also determine the six-nucleotide target site duplication that occurs at the junction between the *gypsy* LTR and the genome upon insertion (Dej et al., 1998). The target site duplication consensus determined from our mapped insertion sites matches the known YRYRYR previously identified for *gypsy* integration sites (Figure 3D) (Dej et al., 1998). To determine the distribution of the insertions sites we divided the largest chromosome arms (3R, 3L, 2R, 2L, X) into roughly 1 megabase bins and counted the number of insertions per bin. Then we plotted the fraction of the total insertions on that chromosome arm in each bin. A plot for the arms of chromosome 3 is shown in figure 3E. The plots of the other chromosomes are in the supplemental figure 3-S1b. At this level of resolution, insertions are detected roughly evenly across the chromosomes.

The feasibility of the system allowed us to test whether TE activity could affect lifespan. We set up three independent cohorts to measure lifespan. The assays were performed at different times of the year. We consistently found that the somatic expression of an active *gypsy* significantly decreased the lifespan of male flies (Fig. 4a). The individual cohorts showed a consistent effect on lifespan and the merged data was used to analyze the effect. A 19% reduction of lifespan in the active *gypsy* male flies is observed compared to parental controls, with a median survival of 70 days and 86 days, respectively. A lifespan effect was also observed in females, surprisingly it was also present in the UAS-*gypsy* parental control (Fig. 4-S1). Interestingly, a molecular assay demonstrates that more detected insertions are present in female UAS-*gypsy* controls than their male equivalents (Fig. 4-S2). An additional molecular assay was done in the *Ubi>gypsy* genotype to look at the distribution of detected insertions between the head and body (Fig. 4-S3). No significant difference was detected in male flies, indicating an equivalent level of insertions throughout somatic tissue. In females, however, a significant bias toward insertions in the body was detected, indicating possible differential expression of UAS-*gypsy* in the mixed tissues. Due to the confounding effects of the system observed in female flies (lifespan defect in parental UAS-*gypsy* control and differential distribution of detected insertions in *Ubi>gypsy*) male flies were used for all following experiments. The lifespan effect on the *Ubi>gypsy* flies only becomes apparent once the flies start to age. At 26 days old the survival curves noticeably separate from the parental controls and calculation of the age specific mortality shows a significant increase in mortality present in 26 to 75 day old animals (Fig. 4b-e).

Ectopic *gypsy* DNA was detected at different ages in the survival curve (5, 14, 30, 50, and 70 days old) with three different primer pairs. In Figure 5a, the recombinant 5' LTR *gypsy* junction is targeted to detect complete ectopic *gypsy* elements. In Figure 5b, the 3' fragment of ectopic *gypsy* is targeted for detection. The 3' fragment comprises the region between the *env* gene and the tag in the 3' LTR. Complete and incomplete *gypsy* elements are quantified by this approach. In Figure 5c, the wildtype *gypsy* env region is targeted. This approach captures both the endogenous and ectopic *gypsy* content in the genome. Of the three approaches, the detection of the 5' LTR *gypsy* junction (Fig. 5a) is the most stringent because only complete *gypsy* elements are detected. This is reflected in the smaller content of ectopic *gypsy* DNA detected compared to the 3' fragment assay which detects both complete and incomplete *gypsy* elements (Fig 5b-c). The three approaches detect a relatively constant level of DNA while the animals are young with a surprising decrease in detection of ectopic *gypsy* DNA in older animals. Interestingly, ectopic *gypsy* RNA expression remains constant throughout the assayed timepoints (Fig. 5d). Although variability increases greatly with age.

The effect on lifespan caused by TE activity could be due to the process of retrotransposition through a DNA intermediate or by disruption of RNA homeostasis. One way to address this is to remove the DNA synthesis step and test if TE RNA presence alone can mediate the decrease in lifespan. This led us to test whether the lifespan effect would be present after deleting the reverse transcriptase (RT) from the UAS-*gypsy* polyprotein. We created a UAS-*gypsy* construct that contains an in-frame deletion in the polyprotein that removes most of the RT (Marlor et al., 1986) and

inserted it in the same attP landing site on chromosome 2 (UAS-*ΔRT*). The deletion of RT in the UAS-*gypsy* transgene prevents the lifespan effect observed when crossed to *Ubi*-gal4 (*Ubi>ΔRT* genotype) (Fig 6a). This is not due to a defect in mRNA levels because RT-qPCR indicates that *Ubi>ΔRT* and *Ubi>gypsy* express the transposon RNA at the same level (Fig. 6b). Consistent with the loss of RT activity, we detect no increase in ectopic *gypsy* 3' DNA in the *Ubi>ΔRT* line despite expressing equivalent levels of mRNA as *Ubi>gypsy* (Fig. 6c). This result indicates that an active RT is required for the observed decrease in lifespan seen when *gypsy* is ectopically expressed in somatic tissue.

271 **Figure 3. NGS mapping of ectopic *gypsy* insertions**

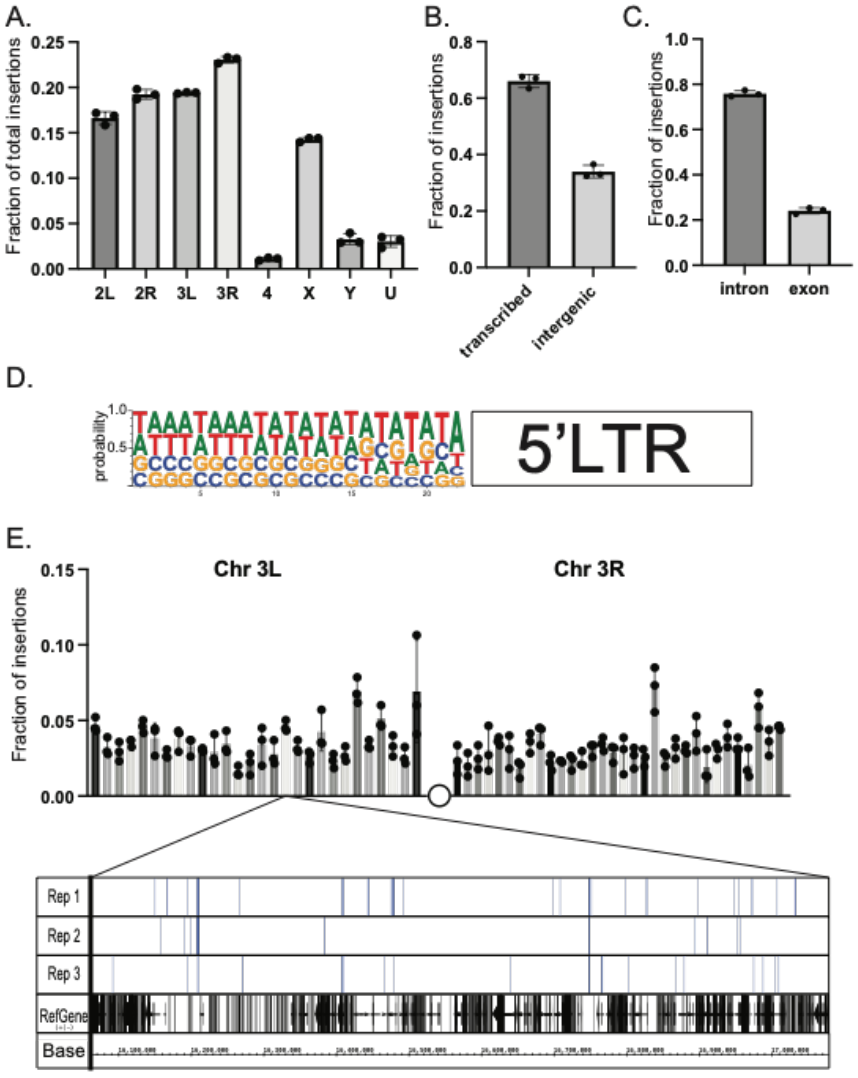

272

273 **Figure 3. NGS mapping of ectopic *gypsy* insertions. A.** The average fraction of total insertions is
274 shown for each chromosome (4, X, Y) or chromosome arm (2L, 2R, 3L, 3R). In addition, the fraction
275 mapping to unplaced contigs is indicated as U. **B.** The fraction of total reads mapping to transcribed
276 regions of the genome and intergenic regions is graphed. **C.** The fraction of insertions that map to
277 the transcribed regions of the genome are subdivided. Insertions mapping to regions annotated as
278 introns or exons is graphed. **D.** The sequences of the junction of the new 5' LTR and the *Drosophila*
279 genome were aligned and used to determine the probability of finding each base at each position.
280 These probabilities are indicated by the size of the letter at each position. **E.** The fraction of
281 insertions that map to each one megabase region of the reference genome for the arms of
282 chromosome 3 are plotted. For illustration, a genome browser view of the 1Mb in Chr3L is shown.
283 The insertion sites in that region for each replicate is indicated. A collapsed track showing genes in
284 that region is also shown. For all histograms, the bars represent the average of three biological
285 replicates. Error bars indicate the standard deviation and the filled circles indicate the individual
286 measurements. Each replicate is a pool of 10 male 14 day-old flies

287 **Figure 4. Ectopic *gypsy* expression decreases lifespan during old age**

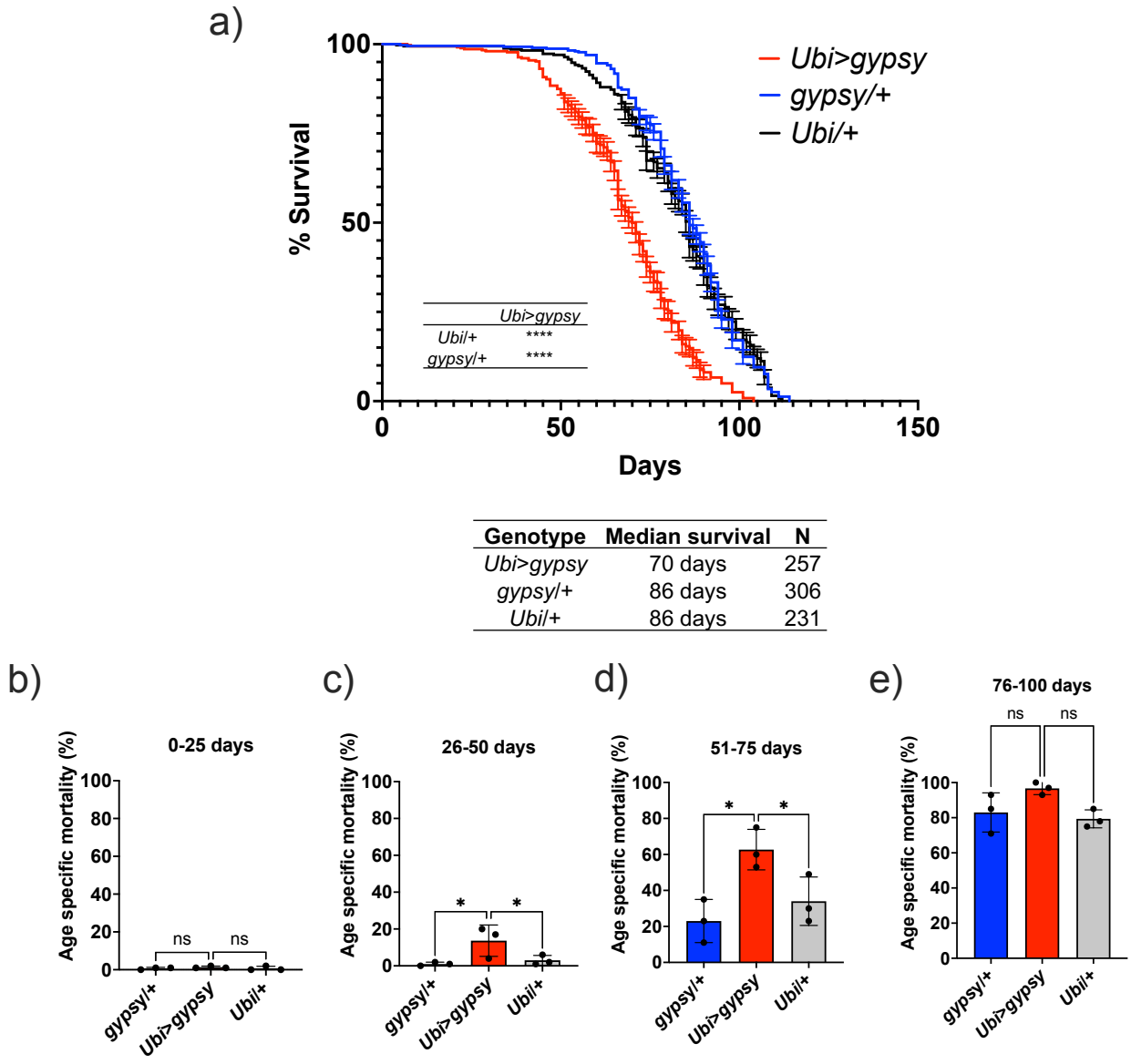

Genotype	Median survival	N
Ubi>gypsy	70 days	257
gypsy/+	86 days	306
Ubi/+	86 days	231

288

289 **Figure 4. Ectopic *gypsy* expression decreases lifespan during old age.** a) Survival curves of
290 male flies expressing *gypsy* under the control of *Ubiquitin* Gal4 (Red) and the parental controls:
291 *gypsy/+* (Blue) and *Ubi/+* (Black). Data represents 3 biological replicates (independent cohorts done
292 at different times of year), error bars SE. **** p value <0.0001, Log-rank test. b-e) Data are
293 represented as means ± SD (individual measurements are shown as dots, age specific mortality was
294 calculated for each cohort independently). One-way ANOVA, adjusted p value: 26-50 days (*gypsy/+*
295 0.047, *Ubi/+* 0.047), adjusted p value 51-75 days (*gypsy/+* 0.015, *Ubi/+* 0.030), ns (not significant).

296 **Figure 5. Ectopic *gypsy* DNA does not increase with age.**

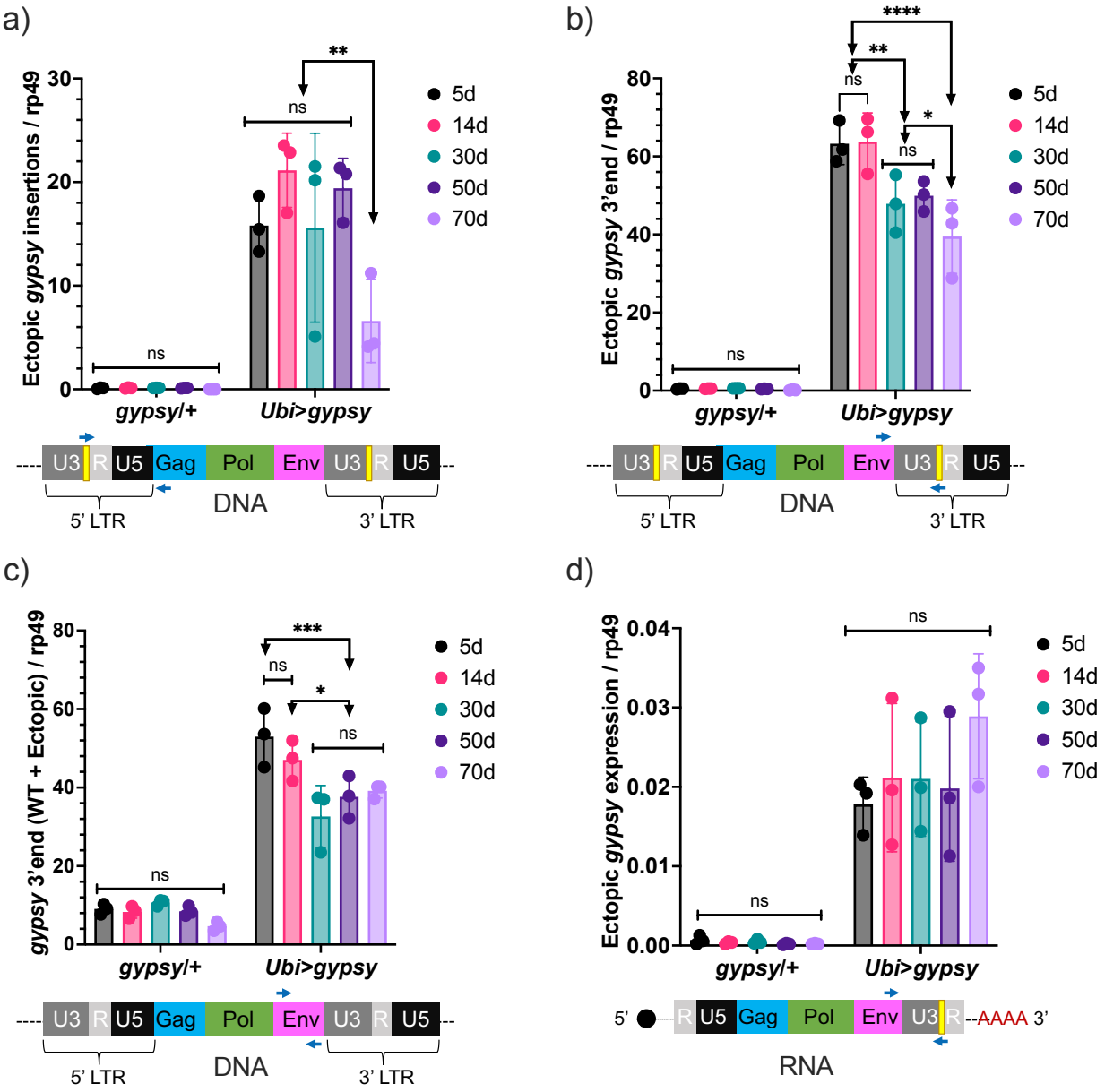

297

298 **Figure 5. Ectopic *gypsy* DNA does not increase with age.** a-c) gDNA qPCR of male flies at
299 different ages (5d, 14d, 30d, 50d and 70d). Data are represented as means ± SD (3 biological
300 replicates, each dot is a pool of 10 flies). 2way ANOVA, **** adjusted p value <0.0001, ** adjusted p
301 value <0.01, * adjusted p value < 0.05. a) Ectopic *gypsy* provirus junctions are detected. b) 3' end of
302 ectopic *gypsy* fragments are detected. c) Wildtype (WT) and ectopic *gypsy env* fragments are
303 detected. d) RT-qPCR of male flies at different ages (5d, 14d, 30d, 50d and 70d). 3' end of ectopic
304 *gypsy* transcript is detected. Data are represented as means ± SD (3 biological replicates, each dot
305 is a pool of 5 flies). 2way ANOVA, not significant (ns).

306 **Figure 6. Decrease in lifespan requires reverse transcriptase activity.**

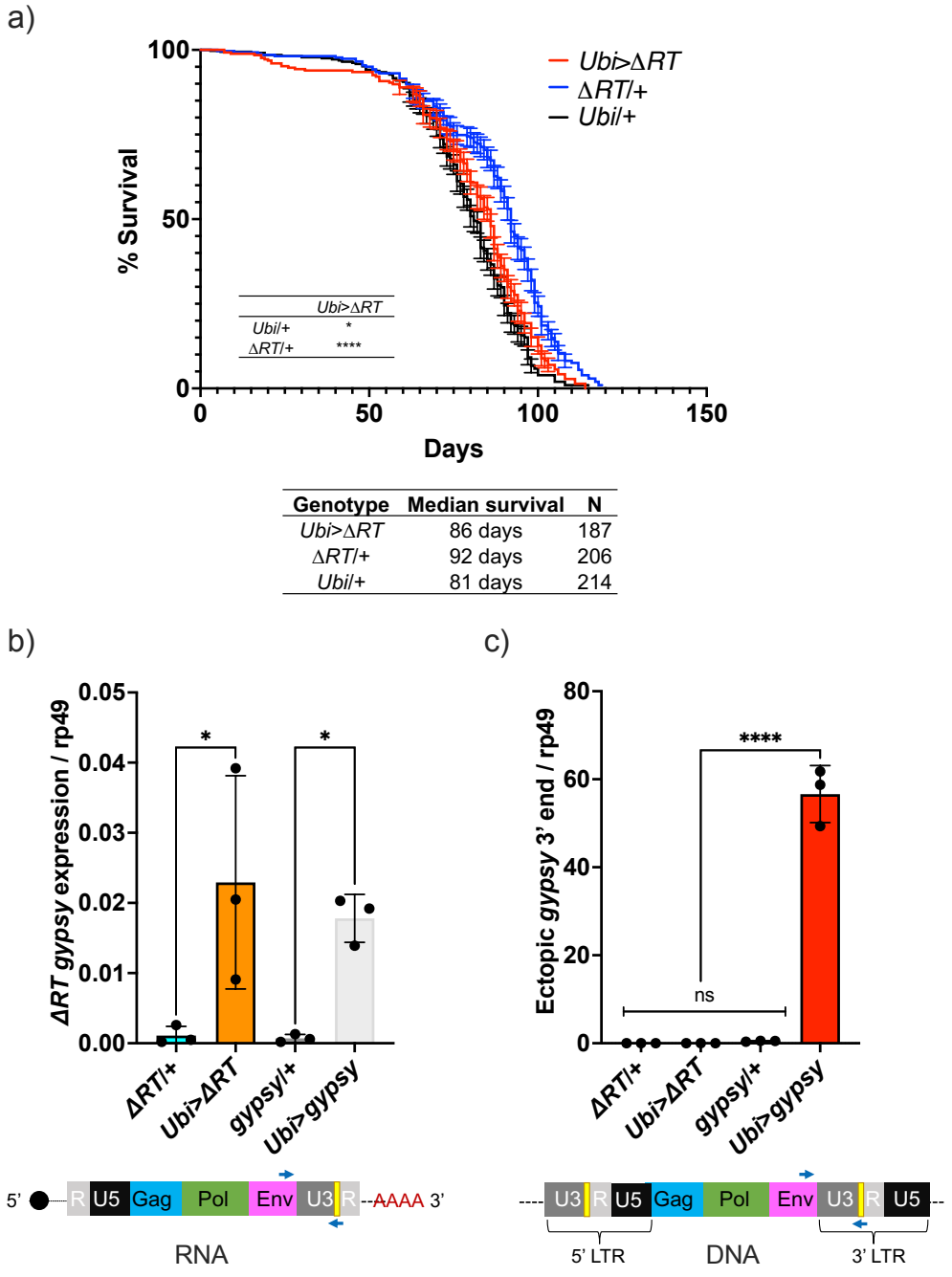

Genotype	Median survival	N
Ubi>ΔRT	86 days	187
ΔRT/+	92 days	206
Ubi/+	81 days	214

307

308 **Figure 6. Decrease in lifespan requires reverse transcriptase activity.** a) Survival curves of male
309 flies expressing *ΔRT gypsy* under the control of *Ubiquitin* Gal4 (Red) and the parental controls: *ΔRT*
310 *gypsy*/+ (Blue) and *Ubi*/+ (Black). Data represents 2 biological replicates (staggered independent
311 cohorts), error bars SE. **** p value <0.0001, * p value 0.016, Log-rank test. b-c) Data are
312 represented as means ± SD (3 biological replicates, each dot is a pool of 5 flies). *gypsy*/+ and
313 *Ubi>gypsy* data are replotted from Fig. 2 b-c, respectively. b) RT-qPCR of 5-day old males. 3' end of
314 ectopic *gypsy* transcript is detected. One-way Anova, *ΔRT*/+ vs. *Ubi>ΔRT* * adjusted p value 0.012,
315 *gypsy*/+ vs. *Ubi>gypsy* * adjusted p value 0.029. c) gDNA qPCR of 5-day old males. 3' end of
316 ectopic *gypsy* fragments is detected. Ordinary one-way Anova, **** adjusted p value <0.0001.

317 To determine if the decrease in lifespan of the active *gypsy* flies was
318 accompanied by an acceleration of aging associated phenotypes, we decided to test if
319 the ectopic expression of the *gypsy* TE resulted in the early emergence of any aging
320 hallmarks. In particular, we focused on four different phenotypes that appear in normal
321 aging flies (decreased resistance to dietary paraquat (Arking et al., 1991), decline in
322 negative geotaxis (Rhodenizer et al., 2008), decrease of total activity (Sun et al., 2013)
323 and disruption of circadian phenotypes (Curran et al., 2019; Rakshit et al., 2012).

324 For the paraquat resistance assays, 5, 15, 30 and 50 day old flies were exposed
325 to 20 mM paraquat. As expected, resistance to paraquat exposure decreased with age
326 in all genotypes (Fig. 7a). Interestingly, the survival curve of the 5-day old active *gypsy*
327 flies mimicked that of the 15-day old parental control curves. Meanwhile the 15-day old
328 active *gypsy* flies had a significant decrease in resistance to paraquat exposure when
329 compared to age matched parental controls. However, once the flies are 30 and 50
330 days old it appears TE activity can no longer exacerbate the oxidative stress survival as
331 experimental and control flies die at a similar rate.

332 We also tested total activity as well as other well-characterized circadian
333 phenotypes such as their ability to anticipate day and night, strength of their free-
334 running conditions, or periodicity. Briefly, we placed 20, 30, or 40 day old flies into
335 *Drosophila* Activity Monitors and recorded their total activity for over 10 days at 25°C in
336 12:12 LD conditions. We did not find any significant decrease in the overall activity
337 levels of the active *gypsy* flies compared to their parental controls at any of the
338 assessed times (Fig. 7-S1). Simultaneously, a separate group of flies was entrained for

339 3 days to the same 12:12 LD conditions and then placed in free-running conditions in
340 constant darkness (DD) to assess the strength of the endogenous clock on these flies.
341 While no significant effect was found in their periodicity, the rhythmicity levels of the flies
342 overexpressing *gypsy* was affected compared to those of their age-matched controls.
343 84-97% of the control flies were rhythmic at all the assessed ages, whereas only 73-
344 77% of the flies with ectopic expression of the TE remain rhythmic (Fig. 7b). Indeed,
345 these flies also display a significant decline in their rhythmicity index throughout the
346 assessed ages which does not happen in the control flies (Fig. 7c).

347 Finally, we also tested the ability of the flies with ectopic *gypsy* expression to
348 move vertically when startled by performing a negative geotaxis assay. Briefly, we
349 tapped the flies and recorded their location within a graduated cylinder for the following
350 15s. We focused on the UAS parental control to select a height and time threshold
351 optimal across different experimental ages (Fig. 7-S2). As a result and to capture
352 possible subtle differences between the young flies and get a robust data capture even
353 in older ages, we focused on the percentage of flies that climbed above the 7.5 cm
354 threshold after 5 and 10 seconds. We examined the climbing ability of the active *gypsy*
355 flies at four different ages (7d, 14d, 35d, 56d). As expected, we observed a decay of
356 negative geotaxis with age. However, we did not detect any accelerated decay in the
357 *gypsy* expressing flies when compared to parental controls (Fig. 7-S3).

Figure 7. *gypsy* activity accelerates a subset of aging phenotypes.

a)

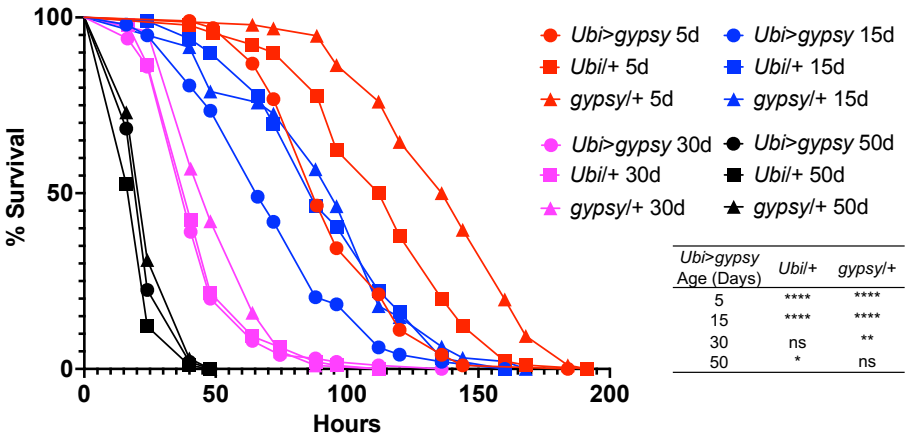

Ubi>gypsy Age (Days)	Ubi/+	gypsy/+
5	****	****
15	****	****
30	ns	**
50	*	ns

b)

Genotype	20 days		30 days		40 days	
	R % (n)	Period (SEM)	R % (n)	Period (SEM)	R % (n)	Period (SEM)
gypsy/+	97 (31)	24.0 (0.19)	95 (22)	23.9 (0.11)	84 (25)	24.1 (0.11)
Ubi>gypsy	73 (22)	23.5 (0.16)	77 (22)	23.8 (0.28)	75 (12	24.2 (0.55)
Ubi/+	86 (28)	23.8 (0.11)	92 (24)	24.11 (0.14)	91 (11)	23.9 (0.19)

c)

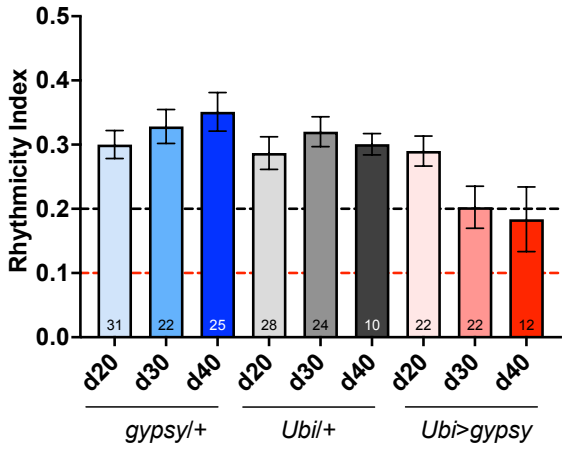

Figure 7. *gypsy* activity accelerates a subset of aging phenotypes. a) Survival curves of male flies after exposure to 20mM paraquat at different ages (Red = 5d, Blue = 15d, Magenta = 30d, and Black = 50d). Experimental flies expressing *gypsy* under the control of *Ubiquitin* Gal4 are represented as circles. The parental controls *Ubi/+* and *gypsy/+* are denoted squares and triangles, respectively. Statistical significance is indicated on graph. * p value 0.013, ** p value 0.006,**** p value <0.0001, Log-rank test. b) Summary table of the percentage of rhythmic flies (R %) and their period in DD. c) Rhythmicity levels of each genotype across the assessed ages (±SEM). *gypsy/+* control, *Ubi>gypsy* experimental, and *Ubi/+* control flies are represented in blue, red, and grey, respectively. The black and red dotted lines mark the thresholds between what are considered highly (RI>0.2) and weakly rhythmic, and arrhythmic flies (RI<0.1). The number at the bottom of each column indicates the n.

Having created a system in which we can regulate the activity of a particular TE (*gypsy*) and having reported the effects of its accumulation upon lifespan and other aging hallmarks, we went back to our original question regarding the role of FOXO on a specific TE. The *Ubi*-gal4 and UAS-*gypsy* lines were crossed to a UAS-*FOXO* line (Slack et al., 2011) to increase *dFOXO* expression in the animals. This leads to a 32% increase in the level of *dFOXO* mRNA in these animals (Fig. 8a). We find that increased expression of *dFOXO* can rescue the effect on lifespan due to *gypsy* activity. The 19% decrease in lifespan reported in Fig. 4a is reduced to 8% when compared to the UAS control and the lifespan matches the gal4 control (Fig. 8b). Importantly, the effect is not simply due to a prevention of ectopic *gypsy* mRNA expression as the transcript remains significantly induced in the *dFOXO* overexpressing flies (Fig. 8c).

382 **Figure 8. Increasing FOXO activity can rescue longevity effect.**

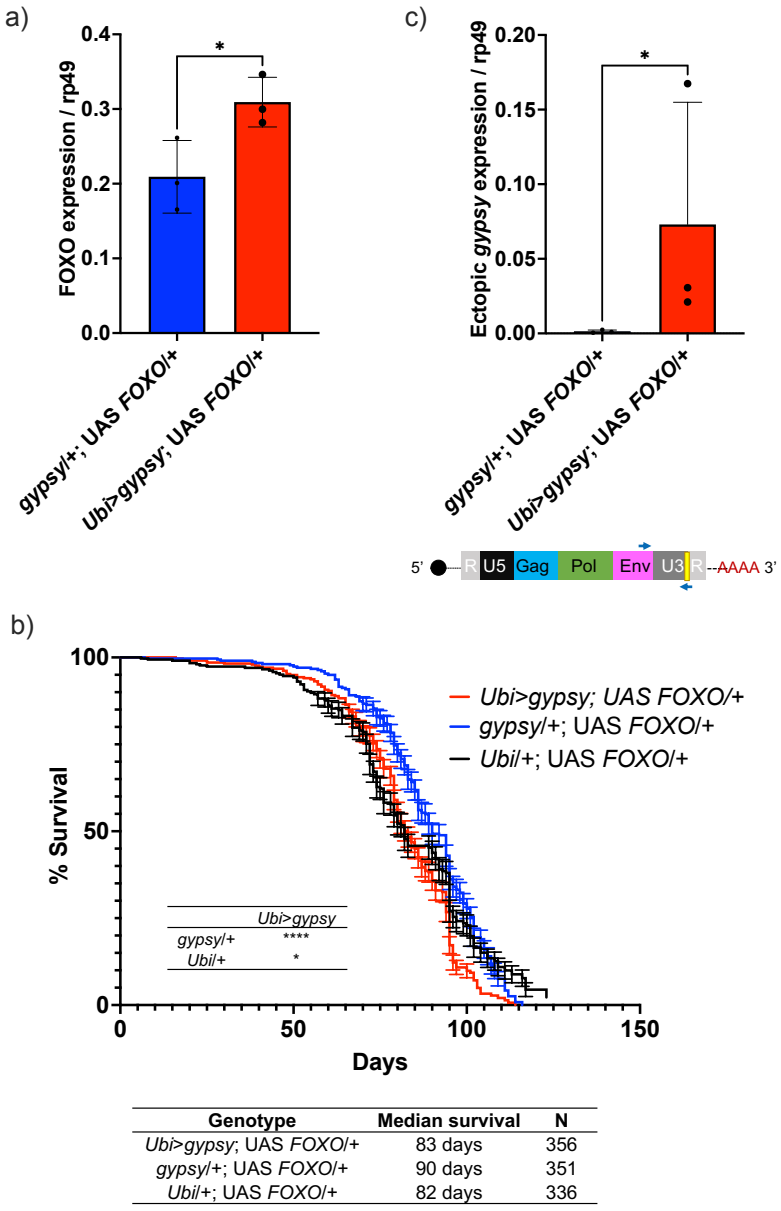

Genotype	Median survival	N
Ubi>gypsy; UAS *FOXO*/+	83 days	356
gypsy/+; UAS *FOXO*/+	90 days	351
Ubi/+; UAS *FOXO*/+	82 days	336

383

384 **Figure 8. Increasing FOXO activity can rescue longevity effect.** a) *dFOXO* exon 8 is detected.
385 RT-qPCR of 5-day old males. Data are represented as means ± SD (3 biological replicates, each dot
386 is a pool of 5 flies). One-tailed t test, * p value 0.021. b) Survival curves of male flies expressing
387 *gypsy* and *dFOXO* under the control of *Ubiquitin* Gal4 (Red line) and the parental controls: *Ubi*/+;
388 UAS-*FOXO*/+ (Black) and *gypsy*/+; UAS-*FOXO*/+ (Blue). Data represents 2 biological replicates,
389 error bars SE. * 0.018 p value, **** p value <0.0001, Log-rank test. c) 3' end of ectopic *gypsy*
390 transcript is detected. RT-qPCR of 5-day old males. Data are represented as means ± SD (3
391 biological replicates, each dot is a pool of 5 flies) One tailed Mann-Whitney test, a non-parametric
392 test, was best suited to fit the tailed distribution of the data, * p value 0.05.

DISCUSSION

Aging can be described as a systemic breakdown due to the accumulation of different stress conditions (López-Otín et al., 2013). The stress response transcription factor FOXO can promote longevity by helping the cell respond to a myriad of conditions: oxidative stress, heat shock, virus infection and defects in protein homeostasis to name a few (Donovan & Marr, 2016; Martins et al., 2016; Spellberg & Marr, 2015). Whether FOXO can protect from the detrimental effects of TE activity on lifespan is an open question.

To begin to investigate this question we measured TE expression with age in dFOXO null and isogenic wt flies. Previous studies of wt animals report both increased and decreased TE mRNA levels with age (Chen et al., 2016; LaRocca et al., 2020). In one study of the female fatbody (5d vs 50d), researchers observed significant increases in 18 TE expression and decreases of 18 TE out of the 111 detected (Chen et al., 2016). While the total number of TE with detectable mRNA changes is lower in our whole animal study, the fact that we detect both increases and decreases in the wildtype animals is consistent with the fatbody study. In the genetic background used here, we find 18 TE have increased mRNA levels in dFOXO null flies, while only two TE showed increased mRNA in wt. Surprisingly, no TE expression is significantly decreased with age in the dFOXO null flies indicating an increase TE load in aged dFOXO null animals. Further, it suggests that the FOXO null animals are deficient in mounting a response to restrict TE expression.

Each fly strain has a unique set of TE that are capable of being transcribed. Likely due to differences in the TE landscape such as the number and location of individual TE copies in the genome (Rahman et al., 2015). We observed this difference in expressed TEs even when comparing expression in young flies (Fig. 1e.) This agrees with previous work showing supposedly isogenic stocks of *D. melanogaster* can have very different TE landscapes (Rahman et al., 2015). This difference in TE content and expression between our wt and dFOXO null strain makes it difficult to determine the effect of FOXO on individual endogenous TEs.

We created the UAS-*gypsy* system to circumvent the difference in TE landscapes and simultaneously perform a direct assay to determine whether TE activity in somatic tissue can be a causative agent of mortality and aging associated phenotypes. We chose the *gypsy* TE as our model for several reasons. First, because previous work has shown that *gypsy* insertions increase during aging, so this retrotransposon is relevant in the natural condition (Y.-H. Chang et al., 2019; Li et al., 2013). Second, a full-length clone of *gypsy* is available and it has been shown to be active and capable of transposition (Bayev et al., 1984). And lastly, the presence of only one full length copy of *gypsy* in the *D. melanogaster* reference genome (Kaminker et al., 2002) suggests a low copy number and mitigates possible unintended trans effects between the endogenous and ectopic TE. To further separate our ectopic TE, a unique 3' sequence tag was inserted. This allows the detection and differentiation of *gypsy* mRNA and DNA content derived from our ectopic *gypsy* element.

435 The presence of the sequence tag in the newly formed 5' LTR of new ectopic
436 *gypsy* insertions allowed us to use our targeted sequencing approach to map a large
437 number of individual new *gypsy* insertions derived from the UAS-*gypsy* synthetic TE.
438 The target site duplication matched the site of endogenous *gypsy* elements (Dej et al.,
439 1998) indicating that the UAS-*gypsy* element likely goes through a replication cycle
440 identical to the natural *gypsy* element. The insertions seem to be evenly distributed and
441 map largely to intronic sequences. This may reflect the fact that we can only recover
442 insertions that do not have a dramatic effect on cell growth. Genomes that suffer
443 insertions disrupting genes that are required for cell viability will be lost from the
444 population and will not be recovered. This approach shows that the UAS-*gypsy* element
445 can make an active transposon that can insert at sites across the genome with little
446 chromosomal bias.

447 The induction of TE activity in somatic tissue resulted in a reduction in *D.*
448 *melanogaster* lifespan when compared to parental controls and a significant increase in
449 mortality in middle aged animals. There was a 19% decrease in the lifespan of male
450 animals. Interestingly, the mortality effects of the active TE are only evident in relatively
451 aged animals, despite the fact that the retrotransposon is active during early life. This
452 suggests that the young animals can tolerate expression and insertion of the TE. It is
453 only when the animals begin to age that TE expression becomes a burden and takes a
454 toll. Perhaps it is the combination of the other metabolic and physiological effects of
455 aging with the TE activity that is detrimental. Coincidently, this is also the timeframe that
456 endogenous TE become expressed during normal aging (Li et al., 2013; Yang et al.,
457 2022).

458 The detectable ectopic *gypsy* insertions were quantified to determine if an
459 increase in detected insertions in the active *gypsy* flies would correlate with the
460 decrease in lifespan. Unexpectedly, detectable insertions do not seem to increase with
461 age, despite constant (although much more variable) expression of the transgene as the
462 animals age. In fact, the oldest animals have the lowest detectable insertions. This
463 finding was measured through three different approaches (the 5' new insertion junction,
464 the 3' fragment of ectopic *gypsy*, and the wildtype *gypsy* env gene). All three
465 approaches agree and show a consistent decrease with age of ectopic *gypsy* DNA
466 content. This suggests that unknown mechanisms are acting to clear or at least prevent
467 an increase in TE insertion load. Whether it is at the level of cellular loss or DNA repair
468 remains to be determined.

469 By using a UAS-*gypsy* strain with a defective RT we were able to determine that
470 a functional RT is needed for the TE effect on lifespan. Previous studies have
471 suggested the need for RT to see detrimental TE effects (Gorbunova et al., 2021). The
472 reverse transcriptase inhibitor 3TC extends the life span of a *Dcr-2* null fly strain, which
473 has an increase in TE expression (Wood et al., 2016). The need for a functional RT to
474 decrease lifespan implicates the DNA synthesis step as being detrimental. Because this
475 also prevents downstream steps such as gene disruption through integration and DNA
476 damage from incomplete integration it is not clear what step beyond DNA synthesis is
477 most detrimental. Future experiments using this approach with integrase mutants of
478 *gypsy* may help to answer this question.

The decrease in lifespan also opened the question of whether the active *gypsy* flies were aging more rapidly, and whether accelerated aging phenotypes could be detected. Criteria to determine premature aging and distinguish it from other causes can be summarized as follows (Salk, 2013). It must first be determined that the increase of mortality at younger ages does not alter the shape of the survival curve. An altered shape of the survival curve indicates that the health of the subjects was compromised and the increase in mortality could be due to unforeseen disease or other factors apart from natural aging processes (Piper & Partridge, 2016). Secondly, a proportional progression of all aging phenotypes without induction of disease must also be observed. The shape of the survival curve for the active *gypsy* flies indicated that the flies were healthy and thus the increase in mortality was not due to disease or external factors. The health of the active *gypsy* flies in the face of their increased mortality led us to test if aging associated phenotypes might be proportionally progressing in them. To determine if this was the case, four aging phenotypes were measured to try to detect whether an acceleration in phenotype development with respect to the parental controls was occurring in the active *gypsy* flies.

Not all phenotypes responded the same. Two out of the four phenotypes assayed show an accelerated decay. An active *gypsy* accelerates the decrease in resistance to paraquat of aging flies. Interestingly, this finding parallels the hypersensitivity to oxidative stress observed when *Dcr-2* is mutated (Lim et al., 2011). Perhaps most dramatically, 5-day old animals with an active *gypsy* have the oxidative stress resistance of a 15-day old animal. The animals' rhythmicity is also impacted. In active *gypsy* flies, rhythmicity decays at a slightly faster rate with most animals

becoming only weakly rhythmic by day 30. Other measures of circadian behavior such as total activity and period did not change with an active TE. The decay of locomotor activity also occurred at a rate similar to controls indicating that not all aging phenotypes show an accelerated decay in response to an active TE. The absence of a locomotor defect also parallels what was observed in the *Dcr-2* null fly strain (Lim et al., 2011). The distinct effects an active TE can generate on the aging phenotypes examined implies that the hallmarks of aging are not uniformly affected, and different aging processes might originate or impact a unique subset of hallmarks. We find that an active TE can accelerate a subset of aging phenotypes, and provide evidence that TE are not merely bystanders in the aging process and can behave as causative agents once they are active.

The development and use of a controllable TE expression system with a direct detrimental effect on longevity allowed us to assay whether increasing the activity of the transcription factor dFOXO played a role in promoting longevity in the face of an active TE. We find that mild overexpression of *dFOXO* can rescue the lifespan defect in the active *gypsy* flies. Though the UAS-*gypsy* was active, the decrease in lifespan was almost completely rescued, highlighting dFOXO's ability to prolong lifespan in the face of TE activity. We and others have previously shown that FOXO responds to paraquat induced oxidative stress (Z. Chang et al., 2019; Donovan & Marr, 2016; Wang et al., 2005) and that dFOXO activates the RNAi pathway (Spellberg & Marr, 2015). Both of these responses would enhance the ability of dFOXO to combat the detrimental effect on lifespan caused by an active TE and suggests a potential new role for dFOXO in its vast repertoire to promote longevity (Martins et al., 2016).

MATERIALS AND METHODS

Fly stocks, *D. melanogaster* husbandry and constructs

D. melanogaster stocks and experimental flies were maintained at 25 °C with a 12 h light/dark cycle at controlled relative humidity. Male flies were used for this study. The fly strains used for RNA-seq were dFOXO null ($w^{DAH\ \Delta 94}$) and its isogenic wildtype control w^{DAH}, both have been previously described (Spellberg & Marr, 2015). The UAS-*gypsy* TAG fly strain was created by modifying the plasmid pDM111, which contains an active copy of *gypsy* (Bayev et al., 1984) (a generous gift from the Corces lab). The white marker from pTARG (Egli et al., 2006), and a phiC31 attB site were added to the plasmid and a unique sequence was inserted in the *gypsy* 3'LTR. The 5' LTR of *gypsy* was precisely replaced with the UAS promoter from pUAST (Brand & Perrimon, 1993) such that the start of transcription matched the start for the *gypsy* LTR. For the RT deletion, the UAS-*gypsy* parent plasmid was cut with AflII to create an in frame deletion of most of the RT from the *gypsy* polyprotein (Marlor et al., 1986). The constructs were sent to BestGene Inc (Chino Hills, CA) for injection into *D. melanogaster*. Transgenes were integrated into the VK37 (Venken et al., 2006) attP site (BDSC 9752) using PhiC31 integrase and balanced. The line was then extensively backcrossed into the w^{1118} background. The *Ubi*-Gal4 and UAS-FOXO fly strains were obtained from Bloomington (32551 and 42221, respectively) and crossed for at least 5 generations into the w^{1118} lab stock. The following strains were generated by crosses: w^{1118}; *Ubi>gypsy* (w^{1118}; *UAS-gypsy* mated to w^{1118}; *Ubi-Gal4*), w^{1118}; *Ubi>*Δ*RT* (w^{1118}; Δ*RT* mated to w^{1118}; *Ubi-Gal4*), w^{1118}; *Ubi*/+; *UAS-FOXO*/+ (w^{1118}; *Ubi-Gal4*;+/*TM3* mated to w^{1118}; *UAS-FOXO*), w^{1118}; *Ubi*/*UAS-gypsy*; *UAS-FOXO*/+ and w^{1118}; *UAS-gypsy*/+; *UAS-*

549 *FOXO*/+ (w^{1118}; *Ubi*/+; *UAS-FOXO*/+ mated to w^{1118}; *UAS-gypsy*). All flies used
550 throughout our experimental procedures were placed in the *w1118* genetic background.
551
552 RNA-seq
553 Total RNA from the whole body of 10 male w^{DAH} and dFOXO null ($w^{DAH\ \Delta 94}$) flies was
554 extracted with TRI Reagent at 5 to 6 days and 30 to 31 days old according to the
555 manufacturers protocol (Molecular Research Center, Inc., Cincinnati, OH). To generate
556 RNA-seq libraries, 1 µg of total RNA was used as input for the TruSeq RNA Library
557 Prep Kit v2 (Illumina, Inc., San Diego, CA) and the manufacturer's protocol was
558 followed. Libraries were sequenced on an Illumina NextSeq 500 in 1 x 75 bp mode.
559 Three individually isolated biological replicates were sequenced for each condition.
560
561 Bioinformatics
562 RNA-seq fastq files were uploaded to the public server usegalaxy.org and processed at
563 the Galaxy web platform (Afgan et al., 2018). The tools FASTQ Groomer (Blankenberg
564 et al., 2010) and FastQC (Andrews, 2010) were used for library quality control. To
565 obtain gene counts, the RNA STAR aligner (Dobin et al., 2012) was used to map the
566 sequencing data to both the *D. melanogaster* genome (dm6) and to a TE consensus
567 FASTA file with 176 *Drosophila* TE. The R package DEBrowser (Kucukural et al., 2019)
568 was used for the following procedures: to filter the counts (1 count per million (CPM) in
569 at least 11/12 libraries), 105 TE passed filtering, calculate differential expression and
570 statistical significance with DESeq2 (parameters: 5% false discovery, 1.5 fold, local, no
571 beta prior, LRT), and generate volcano and scatter plots.

572

573 Life Span Assays

574 Life span assays were performed as previously described (Linford et al., 2013). Briefly,
575 newly eclosed flies were mated for 48hr, sorted by gender, and kept at a standard
576 density of 15 flies per vial. Flies were transferred to fresh food every 2-3 days and
577 mortality was recorded. 3 independent biological replicates of at least 100 flies were
578 performed at different times for *Ubi>gypsy*. The age specific mortality rate was
579 calculated by dividing the deaths occurred in a given age group by the size of the
580 population in which the deaths occurred (*Principles of Epidemiology | Lesson 3 -*
581 *Section 3*, 2021). 2 independent biological replicates were performed at different times
582 for *Ubi>gypsy*; UAS-FOXO/+ and *Ubi>ΔRT*. Kaplan-Meier survival curves were
583 generated with GraphPad Prism version 9 (GraphPad Software, San Diego, California
584 USA, www.graphpad.com) and analyzed with the Log Rank test.

585

586 RT-qPCR and genomic DNA qPCR

587 Total RNA or DNA was extracted from the whole body of 5-10 male flies. RNA was
588 extracted with the TRI Reagent according to the manufacturers protocol (Molecular
589 Research Center, Inc., Cincinnati, OH) and genomic DNA as described previously
590 (Aljanabi & Martinez, 1997). cDNA for RT-qPCR was synthesized as previously
591 described (Olson et al., 2013). RT-qPCR and gDNA qPCR were performed as follows:
592 for a 10 µL reaction 2 µL of cDNA or 50ng of DNA were used as template and assayed
593 with SYBR green with the primers in Table 1. For all experiments, three biological

replicates were assayed for each condition and the relative expression was calculated as a fraction of the housekeeping gene Rp49.

Table 1. qPCR Primers.

Target	Forward	Reverse
Tag- Provirus junction	GCCAAGCTCAGAATTAACCC	TGGTGGGTTCAGATTGTTGG
gypsy env – Tag	TACAGCGCACCATCGATACT	GTGAGGGTTAATTCTGAGCTTG
gypsy env	CTCTGCTACACCGGATGAGT	AGTATCGATGGTGCGCTGTA
Rp49	CCACCAGTCGGATCGATATGC	CTCTTGAGAACGCAGGCGACC
FOXO	CACGGTCAACACGAACCTGG	GGTAGCCGTTTGTGTTGCCA

Oligo adenylation

MB1192 was adenylated using recombinant MTH ligase (Zhelkovsky & McReynolds, 2011). 200pmol of oligo was adenylated in a 200µl reaction (50mM Tris 7.5, 10mM MgCl2, 0.1mM EDTA, 0.1mM ATP, 5mM DTT) with 10µl recombinant MTH ligase. The reaction was incubated at 65˚C for 1 hour and terminated by incubation at 85˚C for 15 minutes. 20µg of glycogen was added to the reaction followed by 500µl ethanol. The oligo was placed at -20˚C for 30 minutes and collected by centrifugation. The pellet was resuspended in 100µl 6M GuHCl, 50mM Tris 6.8. 400µl of ethanol was added and the oligo was loaded onto a silica spin column (BioBasic PCR cleanup). The column was washed once with 80% ethanol and then centrifuged until dry. The adenylated oligo was eluted in 40µl TE and quantitated by UV absorbance.

NGS library preparation

To prepare the insertion libraries, 250ng of genomic DNA was digested with the 4-base cutter MnlI (NEB, Ipswich, MA), overnight at 37˚C according to manufacturer's recommendations, to fragment the genome. Additionally, MnlI cuts the UAS-*gypsy*

element 61 times including 17bp from the 5' end of the 3'LTR to limit the recovery of the parental UAS-*gypsy* sequences. The fragmented DNA was purified using a silica-based PCR cleanup kit (Biobasic, Markham, Canada). A biotinylated primer (MB2640) annealing to the TAG sequence was annealed and extended with 20 cycles of linear amplification with pfuX7(Nørholm, 2010) in a 100µl reaction (20mM Tris-HCl pH 8.8 at 25°C, 10mM (NH4)2SO4, 10mM KCl, 2mM MgSO4, 0.1% Triton® X-100, 200µM dNTPs, 0.5µM primer, 5u pfuX7) The reaction was quenched by adding 400µl TENI (10mM Tris 8.0, 1mM EDTA, 25mM NaCl, 0.01% Igepal 630). Biotinylated products were purified using M270 dynabeads (ThermoFisher, Waltham, MA) by incubating the reaction for 30 minutes at room temperature followed by magnetic separation of bound DNA. The beads were washed three times with TENI. Single-stranded biotinylated DNA was purified by incubating the beads with 0.15N NaOH for 15 minutes at room temperature. Beads were washed once more with 0.15N NaOH to remove the non-biotinylated DNA strand. Beads were neutralized by washing two times in TENI and transferred to a new tube. The adenylated MB1192 oligo was ligated to the biotinylated ssDNA on the dynabeads using MTH ligase(Torchia et al., 2008). Beads were resuspended in a 60µl reaction containing 10mM Hepes pH7.4, 5mM MnCl2 and 60pmol adenylated MB1192 oligo. 5µl recombinant MTH RNA ligase was added and the reaction was incubated at 65˚C for 1 hour and terminated by incubation at 85˚C for 15 minutes. The library was amplified by PCR using a primer to the ligated product (MB1019) and a nested primer containing a 5' tail with illumina sequences (MB2669). The individual libraries were amplified by PCR using primers containing attachment

637 sequences (MB583) and barcodes (MB26673 or MB2674 or MB2675). Libraries were
638 sequenced on an illumina Miseq using a PE 150 kit.

639

640 Table 2. Primers for NGS sequencing.

MB2640	Biotin-GTGAGGGTTAATTCTGAGCTTGGC
MB1192	Phos-AGATCGGAAGAGCACACGTCTGA-3' amino blocked
MB1019	TCAGACGTGTGCTCTTCCGATCT
MB2669	CCTACACGACGCTCTTCCGATCTNNNTTCTTCGCGTGGAGCGTTGA
MB583	AATGATACGGCGACCACCGAGATCTACACTCTTTCCCTACACGACGC TCTTCCGATCT
MB2673	CAAGCAGAAGACGGCATACGAGATTCCGAAACGTGACTGGAGTTCAG ACGTGTGCTCTTCCGATCT
MB2674	CAAGCAGAAGACGGCATACGAGATTACGTACGGTGACTGGAGTTCAG ACGTGTGCTCTTCCGATCT
MB2675	CAAGCAGAAGACGGCATACGAGATATCCACTCGTGACTGGAGTTCAG ACGTGTGCTCTTCCGATCT

641

642 Insertion mapping

643 To process the reads, the fastQ file was first separated by illumina barcode. The
644 individual libraries were processed using Galaxy (Afgan et al., 2018). First MB2667
645 primer sequences were removed from read 1 using Trimmomatic (Bolger et al., 2014).
646 Reads containing the *gypsy* LTR were separated using Barcode Splitter. The remaining
647 LTR sequences were removed using cutadapt (Martin, 2011). The reads were filtered
648 for size and then aligned to the UAS-*gypsy* construct. 20-35% of the reads mapped to
649 the original parental UAS-*gypsy*. Unaligned reads were then aligned to the *Drosophila*
650 genome (dm6) using Bowtie2 (Langmead & Salzberg, 2012). PCR duplicates were
651 removed, and the insertion sites were compared to the flybase genespan annotation to
652 identify all insertions in transcribed regions. Insertion sites were compared to the intron
653 annotation for Ensembl for identifying insertions in introns. The reverse complement of
654 the first 22 nucleotides of the deduplicated insertion sites were used to determine the

probability of finding each nucleotide at each position using weblogo3 (Crooks et al., 2004).

Paraquat stress assay

Male flies generated and reared in the same conditions as life span assay flies were fed 20mM paraquat at 5, 15, 30, or 50 days. Briefly, at the specified time point flies were starved for 3-4 hr prior to transfer into a minimal food medium (5% sucrose, 2% agar, water) containing 20mM paraquat. Mortality was recorded in 8 and 16 hr intervals. 95-100 flies were used per genotype/timepoint for all time points except 5 day Ubi/+ which had 90 flies. Kaplan-Meier survival curves were generated with GraphPad Prism version 9 (GraphPad Software, San Diego, California USA) and analyzed with the Log Rank test.

Negative Geotaxis Assay

A negative geotaxis assay based on previously established protocols (Gargano et al., 2005; Madabattula et al., 2015; Tuxworth et al., 2019) was set up to assay experimental and control flies at 7, 14, 35, and 56 days. Briefly, male flies generated and reared in life span assay conditions were used. The same cohort was assayed for all the different time points. The day before the experiment, flies were transferred under light CO2 to fresh food vials (10 flies per vial) and allowed to recover for at least 18 hr. Flies were then taken out of the incubator and allowed to acclimate to room temperature for 1 hr. They were then transferred to a 50 mL graduated glass cylinder (VWR, Radnor, PA) sealed with a cotton plug and allowed to acclimate for 1 min before starting trials. Trials were recorded

on an iPhone X camera (Apple Inc, Cupertino, California) placed 30 cm away from the recording spot. A trial consisted in tapping flies to the base of the cylinder and allowing them to climb for 20 seconds. They were then given 60 seconds to recover before starting the next trial. A total of 5 trials was performed for each vial. 10 vials were assayed per genotype. N = 100. Flies were then transferred to fresh food vials and returned to the incubator. Linear regression was performed in Prism (GraphPad Software, San Diego, California USA, www.graphpad.com) to determine the slope of the curves and any possible significant differences.

Locomotor Activity Analysis

Flies were entrained in 12:12 LD (light-dark) conditions at 25 °C. The locomotor activity of 20, 30, and 40 days old male flies was recorded using the Trikinetics locomotor activity monitor (Waltham, MA). Two sets of experiments were conducted. On one set, flies were maintained in 12:12 LD throughout the whole length of the experiment (10-12 days). The other set, was entrained in 12:12 for 3 days, followed by at least 5 days in constant darkness (DD). Quantification of total activity and the analysis of circadian rhythmicity strength and period were conducted in Matlab using Vecsey's SCAMP (Donelson et al., 2012). Flies with a rhythmicity index (RI) < 0.1 were classified as arrhythmic; ones with RI 0.1-0.2, as weakly rhythmic, while flies with RI >0.2 were considered strongly rhythmic. Only the period of weakly or strongly rhythmic flies were included in the calculation of the free-running period for each genotype. N is included in figure.

Statistics

All statistical analyses, except RNA-seq, were conducted using GraphPad Prism version 9 for Mac (GraphPad Software, San Diego, California USA, www.graphpad.com). Multiple comparisons in the Ordinary one-way and 2way ANOVA were corrected by the two-stage linear step-up procedure of Benjamini, Krieger and Yekutiel with a false discovery rate of 5%.

Materials availability statement

The transgenic fly strains created during this study can be obtained by request to the corresponding author. All next generation sequencing data generated are undergoing submission at the GEO database and will be publicly accessible.

REFERENCES

Afgan, E., Baker, D., Batut, B., van den Beek, M., Bouvier, D., Čech, M., Chilton, J., Clements, D., Coraor, N., Grüning, B. A., Guerler, A., Hillman-Jackson, J., Hiltemann, S., Jalili, V., Rasche, H., Soranzo, N., Goecks, J., Taylor, J., Nekrutenko, A., & Blankenberg, D. (2018). The Galaxy platform for accessible, reproducible and collaborative biomedical analyses: 2018 update. *Nucleic Acids Research*, *46*(W1), W537–W544. https://doi.org/10.1093/nar/gky379

Aljanabi, S. M., & Martinez, I. (1997). Universal and rapid salt-extraction of high quality genomic DNA for PCR-based techniques. *Nucleic Acids Research*, *25*(22), 4692–4693. https://doi.org/10.1093/nar/25.22.4692

Andrews, S. (2010). *FastQC A Quality Control tool for High Throughput Sequence Data*. https://www.bioinformatics.babraham.ac.uk/projects/fastqc/

Arking, R., Buck, S., Berrios, A., Dwyer, S., & Baker, G. T. (1991). Elevated paraquat resistance can be used as a bioassay for longevity in a genetically based long-lived strain of Drosophila. *Developmental Genetics*, *12*(5), 362–370. https://doi.org/10.1002/dvg.1020120505

Bayev, A. A., Lyubomirskaya, N. V., Dzhumagaliev, E. B., Ananiev, E. V., Amiantova, I. G., & Ilyin, Y. V. (1984). Structural organization of transposable element mdg4 from Drosophila melanogaster and a nucleotide sequence of its long terminal repeats. *Nucleic Acids Research*, *12*(8), 3707–3723.

Blankenberg, D., Gordon, A., Von Kuster, G., Coraor, N., Taylor, J., & Nekrutenko, A. (2010). Manipulation of FASTQ data with Galaxy. *Bioinformatics*, *26*(14), 1783^ a1785.

Bolger, A. M., Lohse, M., & Usadel, B. (2014). Trimmomatic: A flexible trimmer for Illumina sequence data. *Bioinformatics (Oxford, England)*, *30*(15), 2114–2120. https://doi.org/10.1093/bioinformatics/btu170

Brand, A. H., & Perrimon, N. (1993). Targeted gene expression as a means of altering cell fates and generating dominant phenotypes. *Development (Cambridge, England)*, *118*(2), 401–415.

740 Calnan, D. R., & Brunet, A. (2008). The FoxO code. *Oncogene*, *27*(16), 2276–2288.
741 https://doi.org/10.1038/onc.2008.21
742 Cecco, M. D., Ito, T., Petrashen, A. P., Elias, A. E., Skvir, N. J., Criscione, S. W., Caligiana, A.,
743 Brocculi, G., Adney, E. M., Boeke, J. D., Le, O., Beauséjour, C., Ambati, J., Ambati, K.,
744 Simon, M., Seluanov, A., Gorbunova, V., Slagboom, P. E., Helfand, S. L., … Sedivy, J. M.
745 (2019). L1 drives IFN in senescent cells and promotes age-associated inflammation.
746 *Nature*, *566*(7742), 73–78. https://doi.org/10.1038/s41586-018-0784-9
747 Chang, Y.-H., Keegan, R. M., Prazak, L., & Dubnau, J. (2019). Cellular labeling of endogenous
748 retrovirus replication (CLEVR) reveals de novo insertions of the gypsy retrotransposable
749 element in cell culture and in both neurons and glial cells of aging fruit flies. *PLOS*
750 *Biology*, *17*(5), e3000278. https://doi.org/10.1371/journal.pbio.3000278
751 Chang, Z., Xia, J., Wu, H., Peng, W., Jiang, F., Li, J., Liang, C., Zhao, H., Park, K., Song, G., Kim, S.,
752 Huang, R., Zheng, L., Cai, D., & Qi, X. (2019). Forkhead box O3 protects the heart against
753 paraquat-induced aging-associated phenotypes by upregulating the expression of
754 antioxidant enzymes. *Aging Cell*, *18*(5), e12990. https://doi.org/10.1111/acel.12990
755 Chen, H., Zheng, X., Xiao, D., & Zheng, Y. (2016). Age-associated de-repression of
756 retrotransposons in the Drosophila fat body, its potential cause and consequence. *Aging*
757 *Cell*, *15*(3), 542–552. https://doi.org/10.1111/acel.12465
758 Chung, W.-J., Okamura, K., Martin, R., & Lai, E. C. (2008). Endogenous RNA Interference
759 Provides a Somatic Defense against Drosophila Transposons. *Current Biology : CB*,
760 *18*(11), 795–802. https://doi.org/10.1016/j.cub.2008.05.006
761 Crooks, G. E., Hon, G., Chandonia, J.-M., & Brenner, S. E. (2004). WebLogo: A sequence logo
762 generator. *Genome Research*, *14*(6), 1188–1190. https://doi.org/10.1101/gr.849004
763 Curran, J. A., Buhl, E., Tsaneva-Atanasova, K., & Hodge, J. J. L. (2019). Age-dependent changes in
764 clock neuron structural plasticity and excitability are associated with a decrease in
765 circadian output behavior and sleep. *Neurobiology of Aging*, *77*, 158–168.
766 https://doi.org/10.1016/j.neurobiolaging.2019.01.025
767 Czech, B., Malone, C. D., Zhou, R., Stark, A., Schlingeheyde, C., Dus, M., Perrimon, N., Kellis, M.,
768 Wohlschlegel, J. A., Sachidanandam, R., Hannon, G. J., & Brennecke, J. (2008). An

769 endogenous small interfering RNA pathway in Drosophila. *Nature*, *453*(7196), 798–802.
770 https://doi.org/10.1038/nature07007
771 De Cecco, M., Criscione, S. W., Peckham, E. J., Hillenmeyer, S., Hamm, E. A., Manivannan, J.,
772 Peterson, A. L., Kreiling, J. A., Neretti, N., & Sedivy, J. M. (2013). Genomes of
773 replicatively senescent cells undergo global epigenetic changes leading to gene silencing
774 and activation of transposable elements. *Aging Cell*, *12*(2), 247–256.
775 https://doi.org/10.1111/acel.12047
776 De Cecco, M., Criscione, S. W., Peterson, A. L., Neretti, N., Sedivy, J. M., & Kreiling, J. A. (2013).
777 Transposable elements become active and mobile in the genomes of aging mammalian
778 somatic tissues. *Aging*, *5*(12), 867–883. https://doi.org/10.18632/aging.100621
779 Dej, K. J., Gerasimova, T., Corces, V. G., & Boeke, J. D. (1998). A hotspot for the Drosophila
780 gypsy retroelement in the ovo locus. *Nucleic Acids Research*, *26*(17), 4019–4025.
781 Dobin, A., Davis, C. A., Schlesinger, F., Drenkow, J., Zaleski, C., Jha, S., Batut, P., Chaisson, M., &
782 Gingeras, T. R. (2012). STAR: ultrafast universal RNA-seq aligner. *Bioinformatics*, *29*(1),
783 15^ a21.
784 Donelson, N., Kim, E. Z., Slawson, J. B., Vecsey, C. G., Huber, R., & Griffith, L. C. (2012). High-
785 Resolution Positional Tracking for Long-Term Analysis of Drosophila Sleep and
786 Locomotion Using the “Tracker” Program. *PLOS ONE*, *7*(5), e37250.
787 https://doi.org/10.1371/journal.pone.0037250
788 Donovan, M. R., & Marr, M. T. (2016). DFOXO Activates Large and Small Heat Shock Protein
789 Genes in Response to Oxidative Stress to Maintain Proteostasis in Drosophila. *The*
790 *Journal of Biological Chemistry*, *291*(36), 19042–19050.
791 https://doi.org/10.1074/jbc.M116.723049
792 Egli, D., Yepiskoposyan, H., Selvaraj, A., Balamurugan, K., Rajaram, R., Simons, A., Multhaup, G.,
793 Mettler, S., Vardanyan, A., Georgiev, O., & Schaffner, W. (2006). A family knockout of all
794 four Drosophila metallothioneins reveals a central role in copper homeostasis and
795 detoxification. *Molecular and Cellular Biology*, *26*(6), 2286–2296.
796 https://doi.org/10.1128/MCB.26.6.2286-2296.2006

Elsner, D., Meusemann, K., & Korb, J. (2018). Longevity and transposon defense, the case of termite reproductives. *Proceedings of the National Academy of Sciences*, *115*(21), 5504–5509. https://doi.org/10.1073/pnas.1804046115

García Guerreiro, M. P. (2012). What makes transposable elements move in the Drosophila genome? *Heredity*, *108*(5), 461–468. https://doi.org/10.1038/hdy.2011.89

Gargano, J. W., Martin, I., Bhandari, P., & Grotewiel, M. S. (2005). Rapid iterative negative geotaxis (RING): A new method for assessing age-related locomotor decline in Drosophila. *Experimental Gerontology*, *40*(5), 386–395. https://doi.org/10.1016/j.exger.2005.02.005

Ghildiyal, M., Seitz, H., Horwich, M. D., Li, C., Du, T., Lee, S., Xu, J., Kittler, E. L. W., Zapp, M. L., Weng, Z., & Zamore, P. D. (2008). Endogenous siRNAs derived from transposons and mRNAs in Drosophila somatic cells. *Science (New York, N.Y.)*, *320*(5879), 1077–1081. https://doi.org/10.1126/science.1157396

Giordani, G., Cavaliere, V., Gargiulo, G., Lattanzi, G., & Andrenacci, D. (2021). Retrotransposons Down- and Up-Regulation in Aging Somatic Tissues. *Cells*, *11*(1), 79. https://doi.org/10.3390/cells11010079

Gorbunova, V., Seluanov, A., Mita, P., McKerrow, W., Fenyö, D., Boeke, J. D., Linker, S. B., Gage, F. H., Kreiling, J. A., Petrashen, A. P., Woodham, T. A., Taylor, J. R., Helfand, S. L., & Sedivy, J. M. (2021). The role of retrotransposable elements in ageing and age-associated diseases. *Nature*, *596*(7870), 43–53. https://doi.org/10.1038/s41586-021-03542-y

Hancks, D. C., Kazazian, H. H., & Jr. (2012). Active human retrotransposons: Variation and disease. *Current Opinion in Genetics & Development*, *22*(3), 191–203. https://doi.org/10.1016/j.gde.2012.02.006

Huang, C. R. L., Burns, K. H., & Boeke, J. D. (2012). Active transposition in genomes. *Annual Review of Genetics*, *46*, 651–675. https://doi.org/10.1146/annurev-genet-110711-155616

Hyun, S. (2017). Small RNA Pathways That Protect the Somatic Genome. *International Journal of Molecular Sciences*, *18*(5). https://doi.org/10.3390/ijms18050912

826 Ivics, Z., & Izsvák, Z. (2010). Repetitive elements and genome instability. *Seminars in Cancer*
827 *Biology*, *20*(4), 197–199. https://doi.org/10.1016/j.semcancer.2010.08.002
828 Jiang, N., Du, G., Tobias, E., Wood, J. G., Whitaker, R., Neretti, N., & Helfand, S. L. (2013). Dietary
829 and genetic effects on age-related loss of gene silencing reveal epigenetic plasticity of
830 chromatin repression during aging. *Aging*, *5*(11), 813–824.
831 https://doi.org/10.18632/aging.100614
832 Kaminker, J. S., Bergman, C. M., Kronmiller, B., Carlson, J., Svirskas, R., Patel, S., Frise, E.,
833 Wheeler, D. A., Lewis, S. E., Rubin, G. M., Ashburner, M., & Celniker, S. E. (2002). The
834 transposable elements of the Drosophila melanogaster euchromatin: A genomics
835 perspective. *Genome Biology*, *3*(12), research0084.1. https://doi.org/10.1186/gb-2002-
836 3-12-research0084
837 Kawamura, Y., Saito, K., Kin, T., Ono, Y., Asai, K., Sunohara, T., Okada, T. N., Siomi, M. C., &
838 Siomi, H. (2008). Drosophila endogenous small RNAs bind to Argonaute 2 in somatic
839 cells. *Nature*, *453*(7196), 793–797. https://doi.org/10.1038/nature06938
840 Kucukural, A., Yukselen, O., Ozata, D. M., Moore, M. J., & Garber, M. (2019). DEBrowser:
841 Interactive differential expression analysis and visualization tool for count data. *BMC*
842 *Genomics*, *20*(1), 6. https://doi.org/10.1186/s12864-018-5362-x
843 Langmead, B., & Salzberg, S. L. (2012). Fast gapped-read alignment with Bowtie 2. *Nature*
844 *Methods*, *9*(4), 357–359. https://doi.org/10.1038/nmeth.1923
845 LaRocca, T. J., Cavalier, A. N., & Wahl, D. (2020). Repetitive elements as a transcriptomic marker
846 of aging: Evidence in multiple datasets and models. *Aging Cell*, *19*(7), e13167.
847 https://doi.org/10.1111/acel.13167
848 Lee, Y. S., Nakahara, K., Pham, J. W., Kim, K., He, Z., Sontheimer, E. J., & Carthew, R. W. (2004).
849 Distinct Roles for Drosophila Dicer-1 and Dicer-2 in the siRNA/miRNA Silencing
850 Pathways. *Cell*, *117*(1), 69–81. https://doi.org/10.1016/S0092-8674(04)00261-2
851 Li, W., Prazak, L., Chatterjee, N., Grüninger, S., Krug, L., Theodorou, D., & Dubnau, J. (2013).
852 Activation of transposable elements during aging and neuronal decline in Drosophila.
853 *Nature Neuroscience*, *16*(5), 529–531. https://doi.org/10.1038/nn.3368

Lim, D.-H., Oh, C.-T., Lee, L., Hong, J.-S., Noh, S.-H., Hwang, S., Kim, S., Han, S.-J., & Lee, Y. S. (2011). The endogenous siRNA pathway in Drosophila impacts stress resistance and lifespan by regulating metabolic homeostasis. *FEBS Letters*, *585*(19), 3079–3085. https://doi.org/10.1016/j.febslet.2011.08.034

Linford, N. J., Bilgir, C., Ro, J., & Pletcher, S. D. (2013). Measurement of Lifespan in Drosophila melanogaster. *Journal of Visualized Experiments : JoVE*, *71*. https://doi.org/10.3791/50068

López-Otín, C., Blasco, M. A., Partridge, L., Serrano, M., & Kroemer, G. (2013). The Hallmarks of Aging. *Cell*, *153*(6), 1194–1217. https://doi.org/10.1016/j.cell.2013.05.039

Madabattula, S. T., Strautman, J. C., Bysice, A. M., O'Sullivan, J. A., Androschuk, A., Rosenfelt, C., Doucet, K., Rouleau, G., & Bolduc, F. (2015). Quantitative Analysis of Climbing Defects in a Drosophila Model of Neurodegenerative Disorders. *Journal of Visualized Experiments : JoVE*, *100*, 52741. https://doi.org/10.3791/52741

Marlor, R. L., Parkhurst, S. M., & Corces, V. G. (1986). The Drosophila melanogaster gypsy transposable element encodes putative gene products homologous to retroviral proteins. *Molecular and Cellular Biology*, *6*(4), 1129–1134. https://doi.org/10.1128/mcb.6.4.1129-1134.1986

Martin, M. (2011). Cutadapt removes adapter sequences from high-throughput sequencing reads. *EMBnet.Journal*, *17*(1), 10–12. https://doi.org/10.14806/ej.17.1.200

Martins, R., Lithgow, G. J., & Link, W. (2016). Long live FOXO: unraveling the role of FOXO proteins in aging and longevity. *Aging Cell*, *15*(2), 196–207. https://doi.org/10.1111/acel.12427

McCLINTOCK, B. (1950). The origin and behavior of mutable loci in maize. *Proceedings of the National Academy of Sciences of the United States of America*, *36*(6), 344–355.

McCullers, T. J., & Steiniger, M. (2017). Transposable elements in Drosophila. *Mobile Genetic Elements*, *7*(3), 1–18. https://doi.org/10.1080/2159256X.2017.1318201

Morley, A. A. (1995). The somatic mutation theory of ageing. *Mutation Research/DNAging*, *338*(1), 19–23. https://doi.org/10.1016/0921-8734(95)00007-S

Mumford, P. W., Romero, M. A., Osburn, S. C., Roberson, P. A., Vann, C. G., Mobley, C. B., Brown, M. D., Kavazis, A. N., Young, K. C., & Roberts, M. D. (2019). Skeletal muscle LINE-1 retrotransposon activity is upregulated in older versus younger rats. *American Journal of Physiology. Regulatory, Integrative and Comparative Physiology*, *317*(3), R397–R406. https://doi.org/10.1152/ajpregu.00110.2019

Nørholm, M. H. (2010). A mutant Pfu DNA polymerase designed for advanced uracil-excision DNA engineering. *BMC Biotechnology*, *10*, 21. https://doi.org/10.1186/1472-6750-10-21

Okamura, K., Ishizuka, A., Siomi, H., & Siomi, M. C. (2004). Distinct roles for Argonaute proteins in small RNA-directed RNA cleavage pathways. *Genes & Development*, *18*(14), 1655–1666. https://doi.org/10.1101/gad.1210204

Olson, C. M., Donovan, M. R., Spellberg, M. J., & Marr, M. T., II. (2013). The insulin receptor cellular IRES confers resistance to eIF4A inhibition. *ELife*, *2*, e00542. https://doi.org/10.7554/eLife.00542

Piper, M. D. W., & Partridge, L. (2016). Protocols to Study Aging in Drosophila. *Methods in Molecular Biology (Clifton, N.j.)*, *1478*, 291–302. https://doi.org/10.1007/978-1-4939-6371-3_18

Principles of Epidemiology | Lesson 3—Section 3. (2021, December 20). https://www.cdc.gov/csels/dsepd/ss1978/lesson3/section3.html

Rahman, R., Chirn, G. W., Kanodia, A., Sytnikova, Y. A., Brembs, B., Bergman, C. M., & Lau, N. C. (2015). Unique transposon landscapes are pervasive across Drosophila melanogaster genomes. *Nucleic Acids Research*, *43*(22), 10655–10672. https://doi.org/10.1093/nar/gkv1193

Rakshit, K., Krishnan, N., Guzik, E. M., Pyza, E., & Giebultowicz, J. M. (2012). Effects of Aging on the Molecular Circadian Oscillations in Drosophila. *Chronobiology International*, *29*(1), 5–14. https://doi.org/10.3109/07420528.2011.635237

Rhodenizer, D., Martin, I., Bhandari, P., Pletcher, S. D., & Grotewiel, M. (2008). Genetic and environmental factors impact age-related impairment of negative geotaxis in Drosophila by altering age-dependent climbing speed. *Experimental Gerontology*, *43*(8), 739–748. https://doi.org/10.1016/j.exger.2008.04.011

Salk, D. (2013). *Werner's Syndrome and Human Aging*. Springer Science & Business Media.

Slack, C., Giannakou, M. E., Foley, A., Goss, M., & Partridge, L. (2011). DFOXO-independent effects of reduced insulin-like signaling in Drosophila. *Aging Cell*, *10*(5), 735–748. https://doi.org/10.1111/j.1474-9726.2011.00707.x

Spellberg, M. J., & Marr, M. T. (2015). FOXO regulates RNA interference in Drosophila and protects from RNA virus infection. *Proceedings of the National Academy of Sciences of the United States of America*, *112*(47), 14587–14592. https://doi.org/10.1073/pnas.1517124112

Sun, Y., Yolitz, J., Wang, C., Spangler, E., Zhan, M., & Zou, S. (2013). Aging Studies in Drosophila melanogaster. *Methods in Molecular Biology (Clifton, N.J.)*, *1048*, 77–93. https://doi.org/10.1007/978-1-62703-556-9_7

Torchia, C., Takagi, Y., & Ho, C. K. (2008). Archaeal RNA ligase is a homodimeric protein that catalyzes intramolecular ligation of single-stranded RNA and DNA. *Nucleic Acids Research*, *36*(19), 6218–6227. https://doi.org/10.1093/nar/gkn602

Treiber, C. D., & Waddell, S. (2017). Resolving the prevalence of somatic transposition in Drosophila. *ELife*, *6*, e28297. https://doi.org/10.7554/eLife.28297

Tuxworth, R. I., Taylor, M. J., Martin Anduaga, A., Hussien-Ali, A., Chatzimatthaiou, S., Longland, J., Thompson, A. M., Almutiri, S., Alifragis, P., Kyriacou, C. P., Kysela, B., & Ahmed, Z. (2019). Attenuating the DNA damage response to double-strand breaks restores function in models of CNS neurodegeneration. *Brain Communications*, *1*(1). https://doi.org/10.1093/braincomms/fcz005

Venken, K. J. T., He, Y., Hoskins, R. A., & Bellen, H. J. (2006). P[acman]: A BAC transgenic platform for targeted insertion of large DNA fragments in D. melanogaster. *Science (New York, N.Y.)*, *314*(5806), 1747–1751. https://doi.org/10.1126/science.1134426

Wang, M. C., Bohmann, D., & Jasper, H. (2005). JNK Extends Life Span and Limits Growth by Antagonizing Cellular and Organism-Wide Responses to Insulin Signaling. *Cell*, *121*(1), 115–125. https://doi.org/10.1016/j.cell.2005.02.030

Weaver. (2008). *Molecular Biology 4th edition by Weaver, Robert F. (2008) Paperback* (4th edition). Mcgraw Hill Higher Education.

940 Wood, J. G., & Helfand, S. L. (2013). Chromatin structure and transposable elements in
941 organismal aging. *Frontiers in Genetics*, *4*, 274.
942 https://doi.org/10.3389/fgene.2013.00274
943 Wood, J. G., Jones, B. C., Jiang, N., Chang, C., Hosier, S., Wickremesinghe, P., Garcia, M.,
944 Hartnett, D. A., Burhenn, L., Neretti, N., & Helfand, S. L. (2016). Chromatin-modifying
945 genetic interventions suppress age-associated transposable element activation and
946 extend life span in Drosophila. *Proceedings of the National Academy of Sciences of the*
947 *United States of America*, *113*(40), 11277–11282.
948 https://doi.org/10.1073/pnas.1604621113
949 Woodruff, R. C., & Nikitin, A. G. (1995). P DNA element movement in somatic cells reduces
950 lifespan in Drosophila melanogaster: Evidence in support of the somatic mutation
951 theory of aging. *Mutation Research/DNAging*, *338*(1), 35–42.
952 https://doi.org/10.1016/0921-8734(95)00009-U
953 Yang, N., Srivastav, S. P., Rahman, R., Ma, Q., Dayama, G., Li, S., Chinen, M., Lei, E. P., Rosbash,
954 M., & Lau, N. C. (2022). Transposable element landscapes in aging Drosophila. *PLOS*
955 *Genetics*, *18*(3), e1010024. https://doi.org/10.1371/journal.pgen.1010024
956 Zhelkovsky, A. M., & McReynolds, L. A. (2011). Simple and efficient synthesis of 5’ pre-
957 adenylated DNA using thermostable RNA ligase. *Nucleic Acids Research*, *39*(17), e117.
958 https://doi.org/10.1093/nar/gkr544

959

960 **SUPPLEMENTS**

961 **Figure 1 Supplemental 1**. **Differentially expressed TE in wild type**

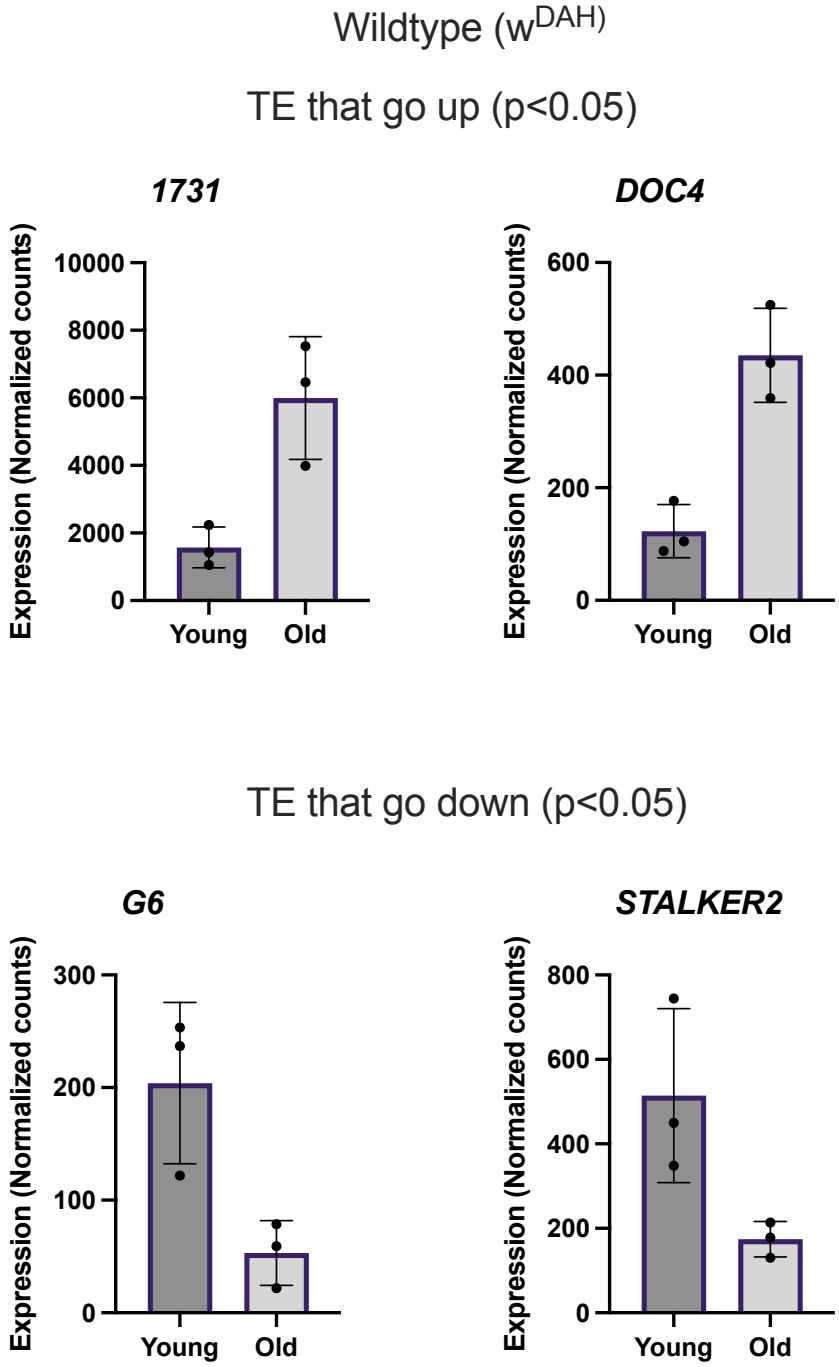

962

963 **Figure 1-S1**. **Differentially expressed TE in wild type.** Median ratio normalized counts by DEseq2
964 of TE differentially expressed with age in wt flies.

965 **Figure 1 Supplemental 2. Differentially expressed TE in FOXO deletion flies.**

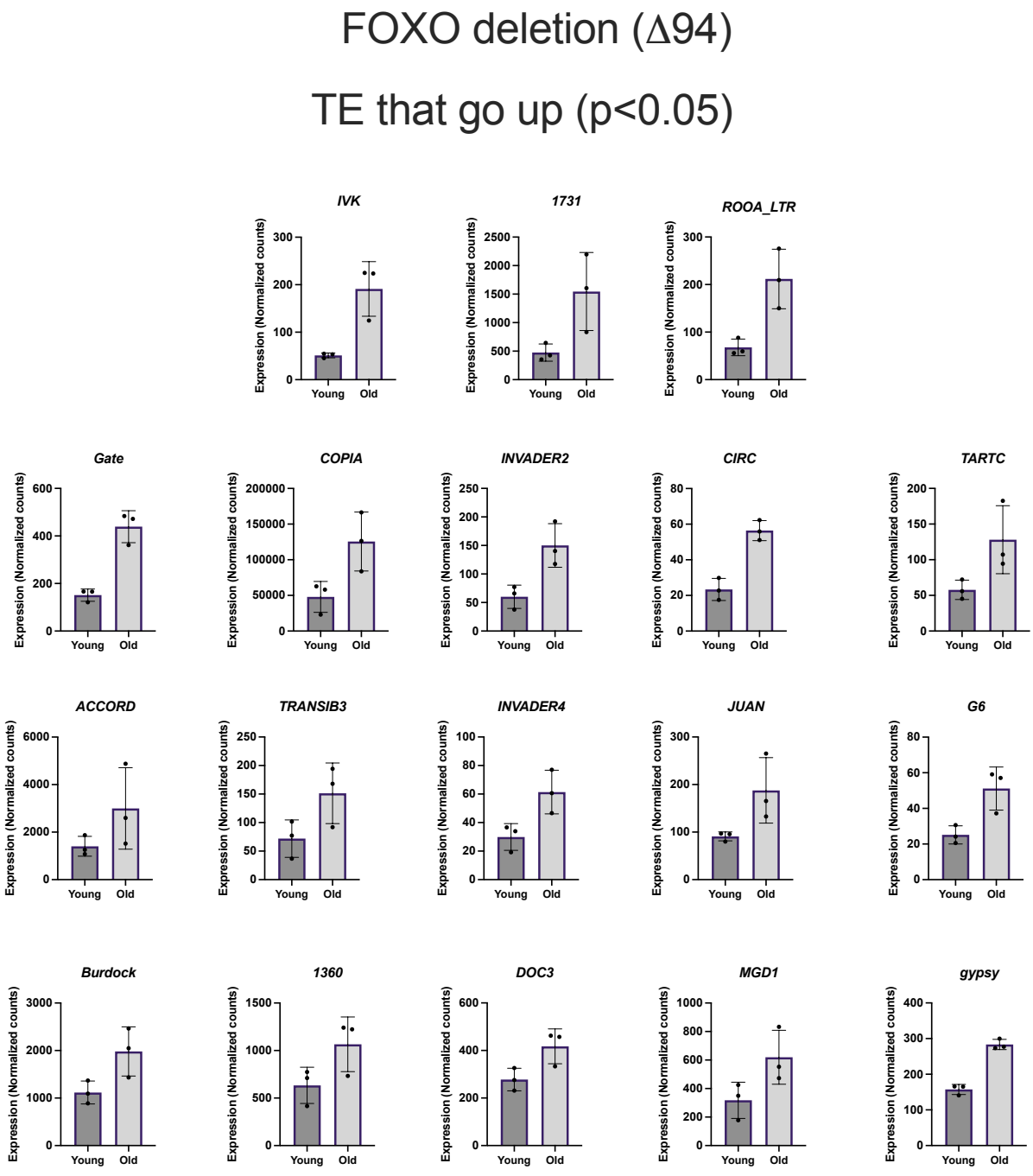

966

967 **Figure 1-S2. Differentially expressed TE in FOXO deletion flies.** Median ratio normalized counts
968 by DEseq2 of TE differentially expressed with age in FOXO deletion flies.

969 **Figure 3 – Supplemental 1. NGS mapping of ectopic *gypsy* insertions.**

a)

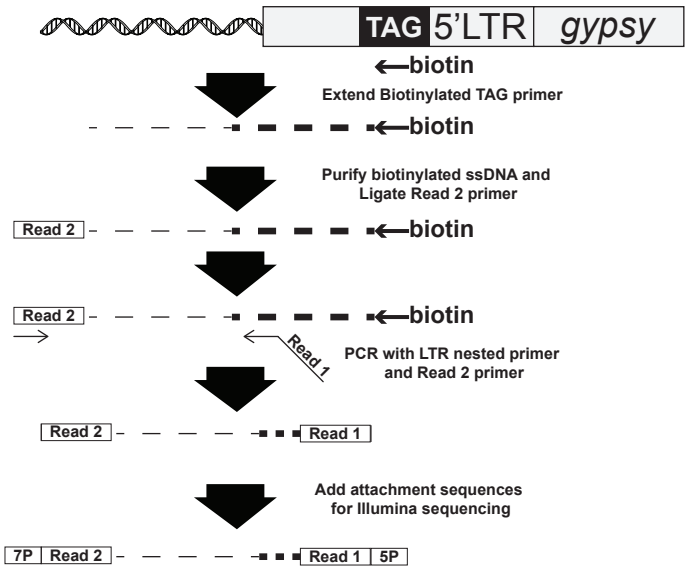

970

b)

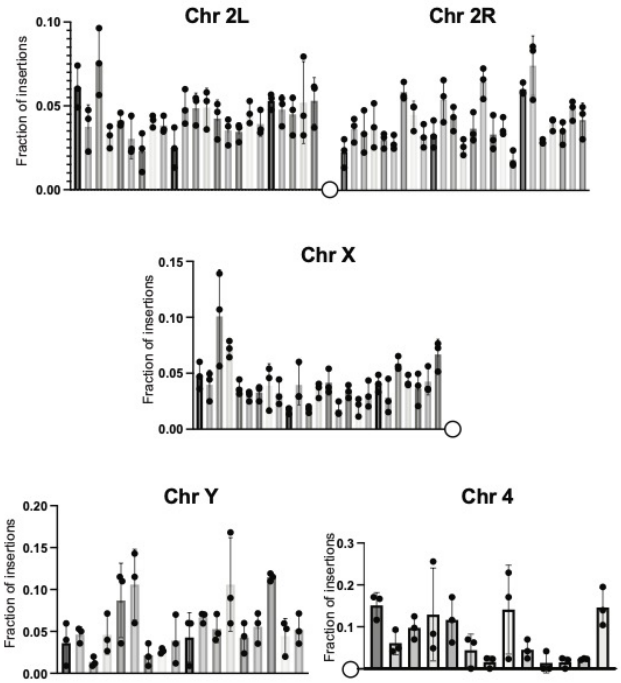

971

972 **Figure 3-S3. NGS mapping of ectopic *gypsy* insertions.** a) Schematic of targeted sequencing
973 approach to map 5' junctions. b) The fraction of insertions that map to each one megabase region of
974 the reference genome for the arms of chromosome 2 and the X chromosome are plotted. For the Y
975 chromosome, each bin represents 200K bases. For the chromosome 4, each bin represents 100K
976 bases. For all histograms, the bars represent the average of three biological replicates. Error bars
977 indicate the standard deviation and the filled circles indicate the individual measurements.

978 **Figure 4 Supplemental 1. Female parental UAS-*gypsy* control has shortened**
979 **lifespan.**

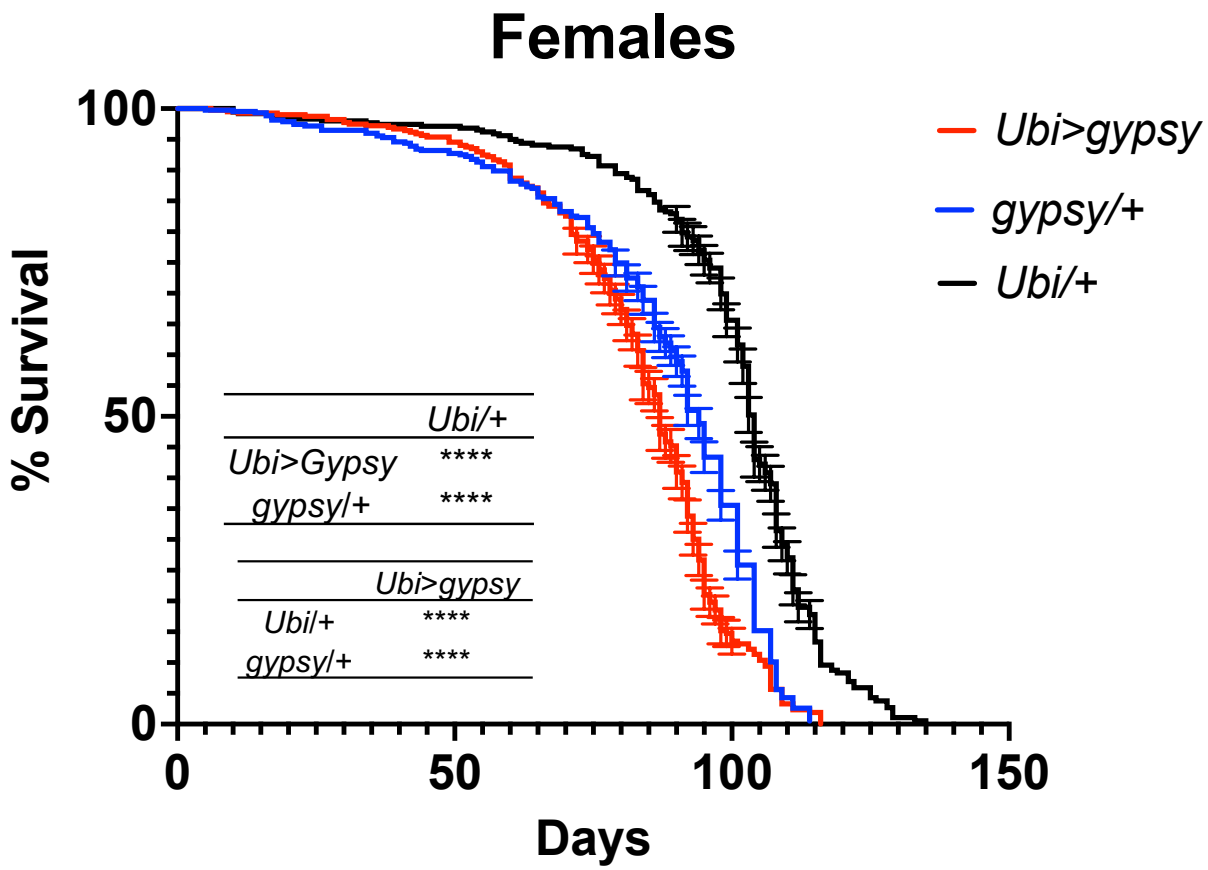

Genotype	Median survival	N
Ubi>gypsy	87 days	257
gypsy/+	94 days	306
Ubi/+	104 days	231

980

981 **Figure 4-S1. Female parental UAS-*gypsy* control has shortened lifespan.** a) Survival curves of
982 female flies expressing *gypsy* under the control of *Ubiquitin* Gal4 (Red) and the parental controls:
983 *gypsy/+* (Blue) and *Ubi/+* (Black). Data represents 3 biological replicates (independent cohorts done
984 at different times of year), error bars SE. **** p value <0.0001, Log-rank test.

985 **Figure 4 Supplemental 2. Male vs female parental UAS *gypsy* control.**

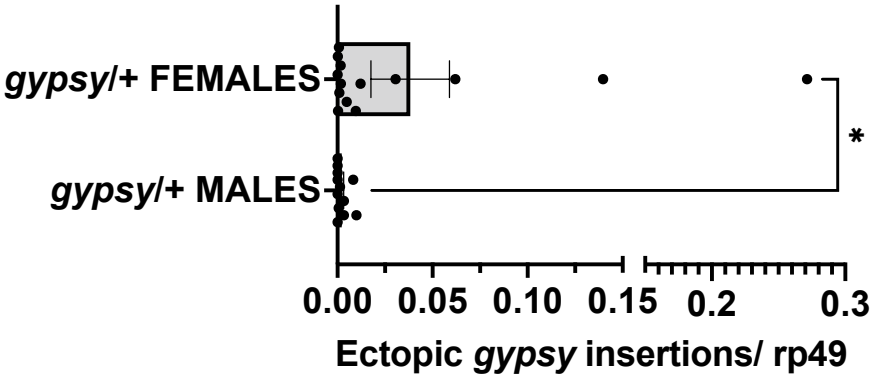

986

987 **Figure 4-S2. Male vs female parental UAS *gypsy* control.** Ectopic *gypsy* provirus insertion
988 junctions are detected. Data are represented as means ± SEM. *gypsy*/+ gDNA from dead flies
989 across the whole lifespan curve was assayed. All dead flies were assayed. Each dot represents a
990 pool of 5-10 dead flies. Two tailed Mann-Whitney test, * p value 0.0177. Male n=12 pools. Female n
991 = 14 pools.

992 **Figure 4 Supplemental 3. Head vs body *gypsy* parental control.**

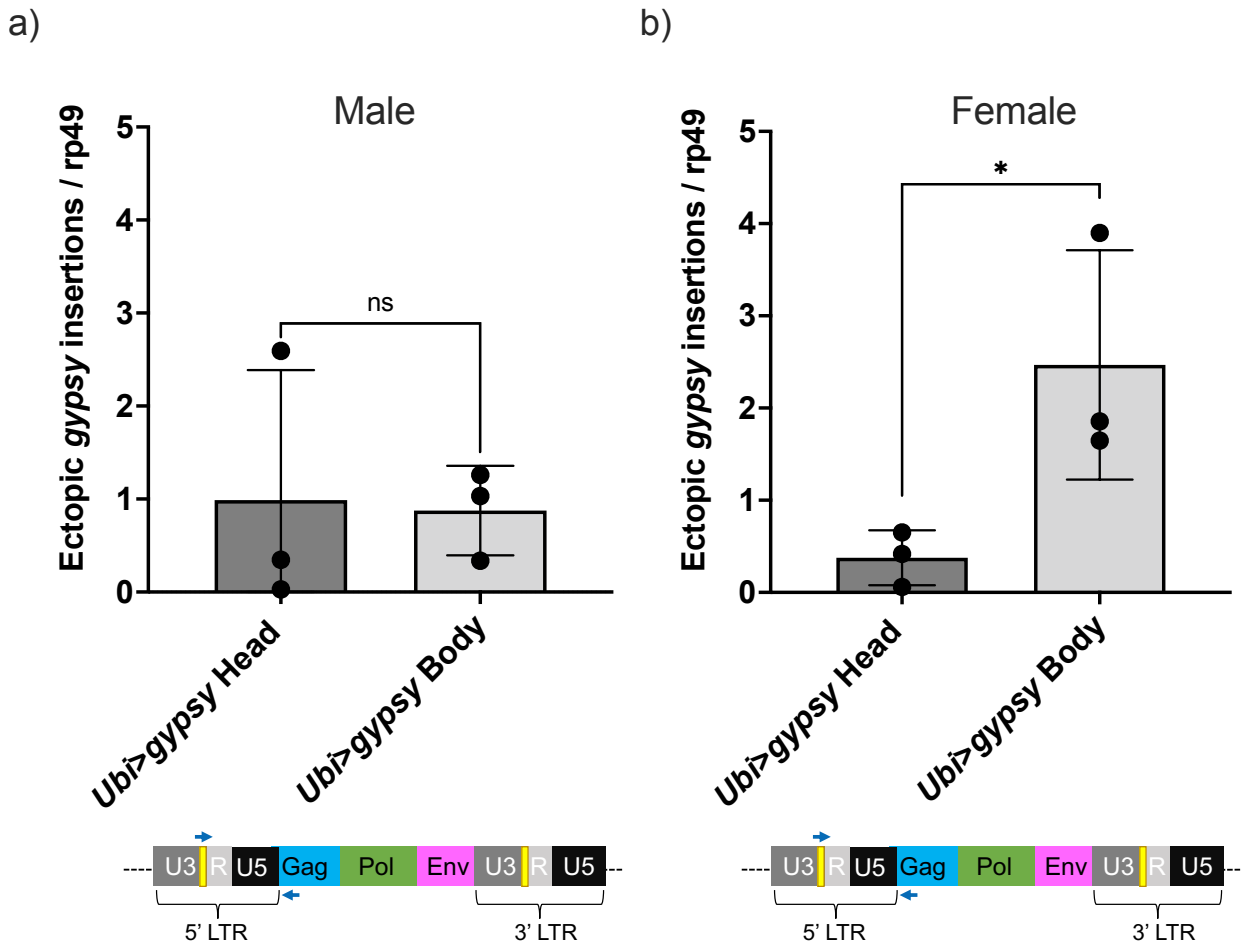

993

994 **Figure 4-S3. Head vs body *gypsy* parental control.** a-b) Ectopic *gypsy* provirus insertion junctions
995 are detected. Data are represented as means ± SD (3 biological replicates, each dot represents a
996 pool of gDNA from 15-20 14d-old heads or bodies). a) Males. 2 tailed unpaired t test, ns p value
997 >0.9. b) Females. 2 tailed unpaired t test, * p value 0.047.

998 **Figure 7 Supplemental 1. Total activity**

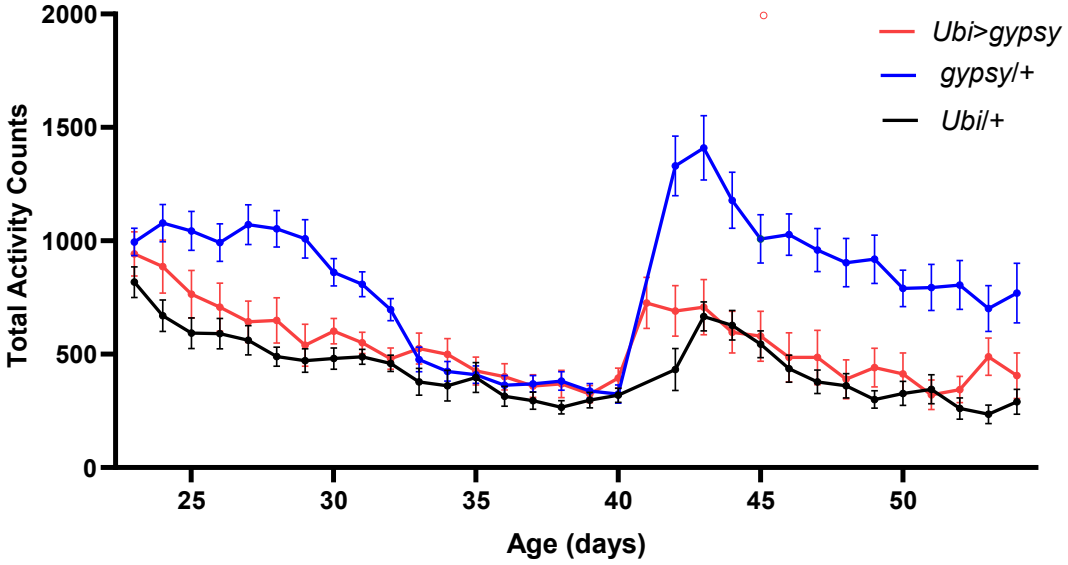

999

1000 **Figure 7-S1. Total activity counts of each genotype *per* day under 12:12 LD conditions.** The
1001 sudden increase in activity around day 40 corresponds with the start of a new recording. UAS-
1002 *gypsy*/+ blue line. *Ubi>gypsy* red line. *Ubi*/+ black line. N=26-32. Data are represented as means ±
1003 SEM.

1004 **Figure 7 Supplemental 2. Negative geotaxis threshold optimization.**

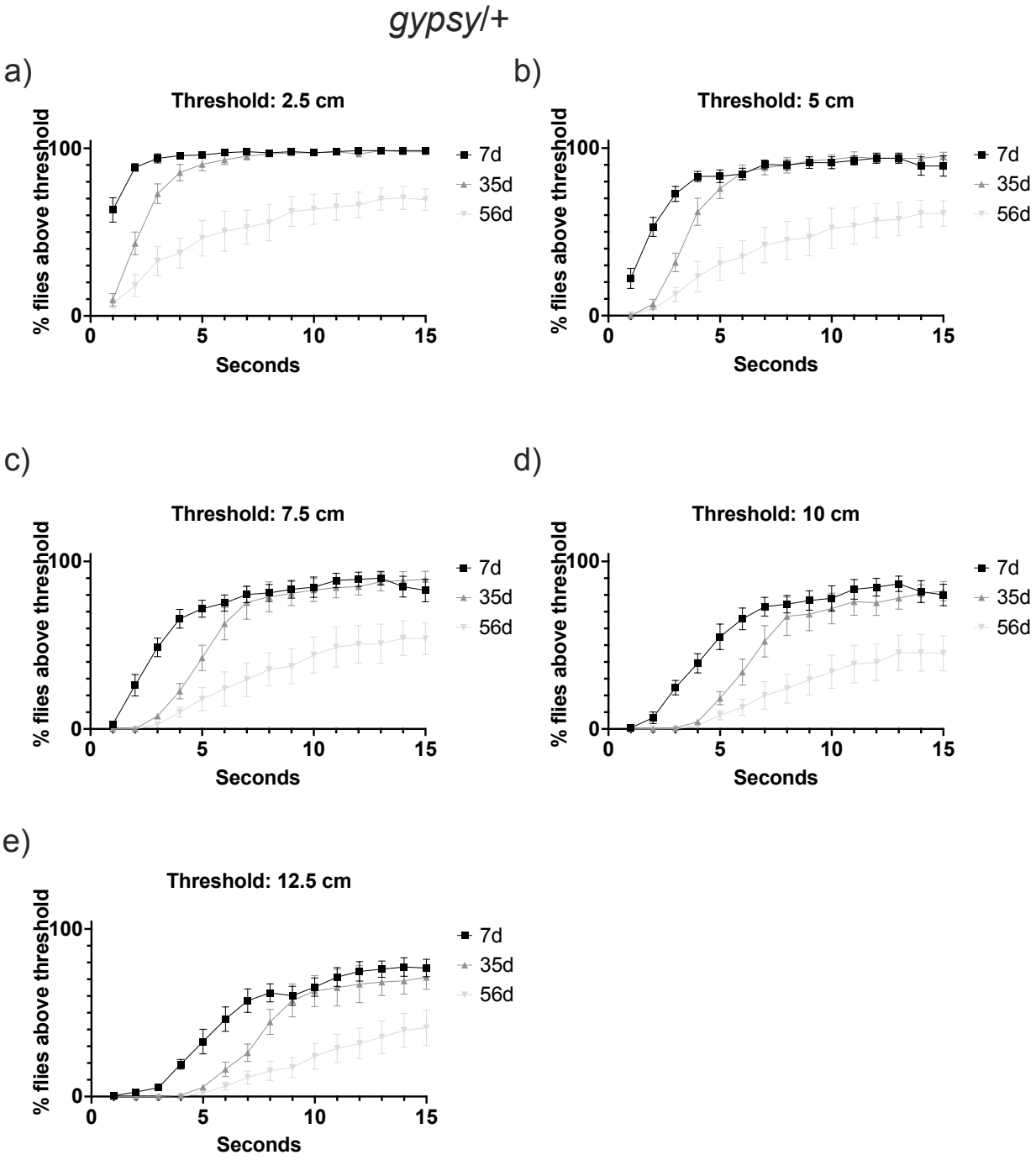

1005
1006 **Figure 7 S2. Negative geotaxis threshold optimization.** Climbing behavior at 3 different ages (7
1007 day old (black square), 35 day old (grey triangle), and 56 day old (light grey inverted triangle) of the
1008 UAS-*gypsy* parental control. Data are represented as means ± SEM (5 biological replicates, 3 trials
1009 each).

1010 **Figure 7 Supplemental 3. Negative geotaxis.**
1011

a)

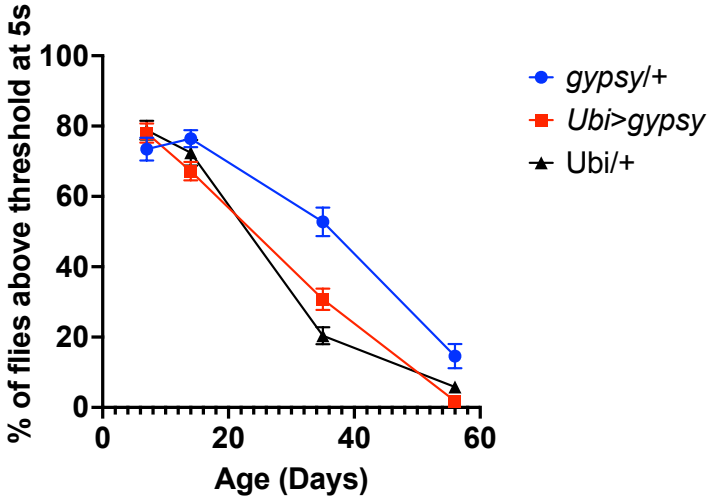

b)

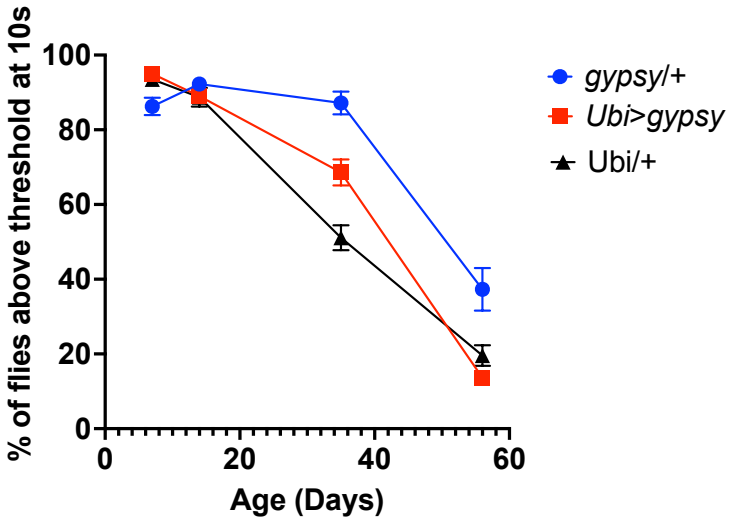

1012
1013 **Figure 7-S3. Negative geotaxis.** Threshold 7.5 cm. Data are represented as means ± SEM (10
1014 biological replicates, 10 male flies each, 5 trials per replicate). *gypsy*/+ blue circles. *Ubi>gypsy* red
1015 squares. *Ubi*/+ black triangles. A) 5 seconds. B) 10 seconds. Slopes were analyzed by simple linear
1016 regression and determined to be not significantly different from each other.

Figure 1-Table supplement 1 (WT). Wild type control TE expression. Counts have been normalized by median ratio normalization in DESeq2. Adjusted p value calculated by DEseq2 is provided.

TE	wt_6d_1	wt_6d_2	wt_5d_3	wt_30d_1	wt_30d_2	wt_30d_3	adjusted p value	Fold Change	Class
17.6	57	108	49	29	100	98	9.97E-01	1.06	Retrotransposon
297	722	1071	787	68	409	684	9.39E-01	0.45	Retrotransposon
412	136	174	95	61	126	238	9.97E-01	1.05	Retrotransposon
1731	1432	2236	1051	3987	6466	7530	2.10E-04	3.81	Retrotransposon
ACCORD	49	436	21	1	40	157	9.97E-01	0.39	Retrotransposon
aurora-element	41	27	27	35	29	28	9.97E-01	0.98	Retrotransposon
BAGGINS	28	43	19	12	31	60	9.97E-01	1.14	Retrotransposon
Beagle	486	391	455	343	400	369	9.97E-01	0.83	Retrotransposon
Beagle2	23	56	11	11	25	54	9.97E-01	0.99	Retrotransposon
Bel	1000	1365	314	254	882	1594	9.97E-01	1.02	Retrotransposon
BLOOD	488	578	505	135	499	381	9.97E-01	0.65	Retrotransposon
BS	63	84	27	26	49	66	9.97E-01	0.81	Retrotransposon
BS3	66	60	23	65	59	52	9.97E-01	1.17	Retrotransposon
Burdock	1044	1138	704	900	1811	1675	9.96E-01	1.52	Retrotransposon
CIRC	43	41	17	14	45	73	9.97E-01	1.30	Retrotransposon
COPIA	78001	138845	60568	95444	238381	250318	6.22E-01	2.11	Retrotransposon
CR1A	333	463	124	142	344	419	9.97E-01	0.98	Retrotransposon
Diver	131	127	19	7	71	121	9.97E-01	0.72	Retrotransposon
DIVER2	62	51	10	4	33	46	9.97E-01	0.68	Retrotransposon
DM_ROO	1320	1461	521	898	1373	1649	9.97E-01	1.19	Retrotransposon
DM88	57	62	16	22	50	66	9.97E-01	1.02	Retrotransposon
DMGYPF1A	777	984	454	311	644	862	9.97E-01	0.82	Retrotransposon
DOC	2501	4171	1162	480	2344	3052	9.97E-01	0.75	Retrotransposon
DOC2	241	303	40	52	151	248	9.97E-01	0.77	Retrotransposon

DOC3	114	134	63	84	146	138	9.97E-01	1.18	Retrotransposon
DOC4	105	177	88	525	422	359	1.00E-05	3.52	Retrotransposon
DOC5	8	18	9	14	26	36	1.00E+00	2.14	Retrotransposon
F-element	392	646	138	74	304	594	9.97E-01	0.83	Retrotransposon
Flea	1122	1506	397	310	1042	1294	9.97E-01	0.87	Retrotransposon
FROGGER	59	62	6	7	42	57	9.97E-01	0.84	Retrotransposon
FW2	38	44	15	19	45	41	9.97E-01	1.08	Retrotransposon
FW3	43	38	27	34	36	42	9.97E-01	1.04	Retrotransposon
G2	87	71	33	28	56	73	9.97E-01	0.82	Retrotransposon
G3	15	21	12	4	22	23	1.00E+00	1.02	Retrotransposon
G4	129	142	74	73	130	160	9.97E-01	1.05	Retrotransposon
G5	57	74	11	27	70	72	9.97E-01	1.19	Retrotransposon
G5A	184	185	155	147	175	218	9.97E-01	1.03	Retrotransposon
G6	122	237	253	22	79	59	8.30E-03	0.26	Retrotransposon
Gate	252	288	69	240	563	881	3.95E-01	2.76	Retrotransposon
GTWIN	28	78	13	36	70	62	9.97E-01	1.40	Retrotransposon
GYPSY10	179	225	102	110	197	228	9.97E-01	1.06	Retrotransposon
GYPSY11	24	20	4	12	11	15	1.00E+00	0.80	Retrotransposon
GYPSY2	29	33	13	23	36	38	9.97E-01	1.26	Retrotransposon
GYPSY4	52	91	33	35	68	81	9.97E-01	1.05	Retrotransposon
GYPSY5	22	33	10	10	38	21	1.00E+00	1.05	Retrotransposon
GYPSY6	25	7	13	17	18	13	1.00E+00	1.04	Retrotransposon
GYPSY8	53	29	17	25	54	70	9.97E-01	1.50	Retrotransposon
GYPSY9	59	56	26	33	52	43	9.97E-01	0.91	Retrotransposon
HeT-A	1110	1252	658	729	1253	1494	9.97E-01	1.15	Retrotransposon
I-element	270	552	105	85	349	509	9.97E-01	1.02	Retrotransposon
Idefix	141	250	86	105	239	309	9.97E-01	1.36	Retrotransposon
INVADER	49	63	18	31	53	66	9.97E-01	1.15	Retrotransposon

INVADER2	47	145	19	22	103	158	9.97E-01	1.34	Retrotransposon
INVADER3	70	123	67	140	127	128	9.23E-01	1.51	Retrotransposon
INVADER4	36	29	10	35	47	73	8.52E-01	2.07	Retrotransposon
IVK	95	167	16	18	156	218	9.97E-01	1.40	Retrotransposon
Jockey	644	705	330	316	556	769	9.97E-01	0.98	Retrotransposon
Jockey_1	282	386	212	263	334	405	9.97E-01	1.14	Retrotransposon
JOCKEY2	219	196	108	201	199	166	9.97E-01	1.08	Retrotransposon
JUAN	87	82	23	17	73	77	9.97E-01	0.87	Retrotransposon
Max-element	2543	2091	1407	2719	2744	3012	9.96E-01	1.40	Retrotransposon
MDG3	288	418	104	143	437	505	9.97E-01	1.34	Retrotransposon
MGD1	298	346	134	214	382	580	9.97E-01	1.51	Retrotransposon
Micropia	19	19	5	11	25	30	1.00E+00	1.52	Retrotransposon
ninja	43	39	26	44	52	67	9.97E-01	1.52	Retrotransposon
OPUS	1991	2046	588	1730	3516	4090	8.73E-01	2.02	Retrotransposon
QBERT	46	51	19	43	73	82	9.97E-01	1.68	Retrotransposon
QUASIMODO	47	53	17	17	39	62	9.97E-01	1.00	Retrotransposon
R1-2	21	23	11	12	11	17	1.00E+00	0.73	Retrotransposon
R1A1-element	7	27	11	28	26	25	1.00E+00	1.73	Retrotransposon
ROOA_LTR	382	444	69	144	454	1048	9.97E-01	1.84	Retrotransposon
ROVER	64	133	106	127	289	348	1.44E-01	2.52	Retrotransposon
Rt1a	32	54	50	11	43	36	9.97E-01	0.67	Retrotransposon
RT1B	179	193	47	110	227	167	9.97E-01	1.20	Retrotransposon
RT1C	24	27	7	17	27	20	1.00E+00	1.07	Retrotransposon
S-element	102	134	37	69	97	136	9.97E-01	1.10	Retrotransposon
S2	21	29	17	25	23	33	1.00E+00	1.20	Retrotransposon
SPRINGER	723	876	409	655	1035	1186	9.97E-01	1.43	Retrotransposon
STALKER2	450	745	348	130	178	214	1.07E-03	0.34	Retrotransposon
TABOR	149	240	54	71	169	258	9.97E-01	1.12	Retrotransposon

TARTC	106	189	51	34	104	141	9.97E-01	0.81	Retrotransposon
TOM1_LTR	72	75	91	110	93	89	9.97E-01	1.23	Retrotransposon
Transpac	569	833	296	273	953	973	9.97E-01	1.29	Retrotransposon
X-ELEMENT	67	115	21	15	58	102	9.97E-01	0.86	Retrotransposon
ZAM	24	41	29	7	34	28	9.97E-01	0.73	Retrotransposon
1360	1126	1263	543	916	1226	1333	9.97E-01	1.18	DNA
BARI1	82	78	45	64	99	77	9.97E-01	1.16	DNA
Hobo	365	463	237	139	384	390	9.97E-01	0.86	DNA
Pogo	720	678	801	792	889	741	9.97E-01	1.10	DNA
HB	161	215	40	53	167	173	9.97E-01	0.94	DNA
FB	200	185	146	197	237	244	9.97E-01	1.27	DNA
Hopper	24	21	19	16	31	22	1.00E+00	1.05	DNA
INE1	164	208	96	104	196	207	9.97E-01	1.08	DNA
MARINER2	97	78	69	104	103	96	9.97E-01	1.24	DNA
P-element	432	405	285	322	421	314	9.97E-01	0.94	DNA
TC1	126	156	29	43	90	147	9.97E-01	0.89	DNA
TC1-2	59	133	55	44	103	161	9.97E-01	1.24	DNA
TRANSIB2	123	102	49	71	115	117	9.97E-01	1.10	DNA
TRANSIB3	90	166	44	136	205	231	8.73E-01	1.90	DNA
TRANSIB4	7	20	9	7	11	20	1.00E+00	1.07	DNA

Figure 1-Table supplement 2 (FOXO null). FOXO null TE expression. Counts have been normalized by median ratio normalization in DESeq2. Adjusted p value calculated by DEseq2 is provided.

TE	Δ94_6d_1	Δ94_6d_2	Δ94_6d_3	Δ94_31d_1	Δ94_31d_2	Δ94_30d_3	adjusted p value	Fold Change	Class
17.6	28	67	58	81	90	73	1.50E-01	1.60	Retrotransposon
297	194	506	164	949	1081	270	1.78E-01	2.66	Retrotransposon
412	125	256	223	284	129	58	6.18E-01	0.78	Retrotransposon
1731	354	427	645	834	1605	2198	5.00E-05	3.25	Retrotransposon
ACCORD	1077	1259	1875	2598	4876	1519	2.47E-02	2.14	Retrotransposon
aurora-element	19	16	22	9	13	22	5.68E-01	0.74	Retrotransposon
BAGGINS	33	33	29	47	40	34	4.82E-01	1.29	Retrotransposon
Beagle	112	211	270	265	328	248	2.41E-01	1.42	Retrotransposon
Beagle2	8	21	25	29	53	22	1.51E-01	1.98	Retrotransposon
Bel	873	732	620	1128	894	1026	1.03E-01	1.37	Retrotransposon
BLOOD	718	1574	1252	1974	1922	1453	1.33E-01	1.51	Retrotransposon
BS	272	288	307	395	355	536	4.52E-02	1.48	Retrotransposon
BS3	47	46	54	41	38	41	5.29E-01	0.81	Retrotransposon
Burdock	888	1094	1369	2049	2463	1434	1.26E-02	1.78	Retrotransposon
CIRC	18	30	23	51	62	56	3.00E-03	2.43	Retrotransposon
COPIA	23126	62779	58084	126439	166397	83807	3.97E-03	2.62	Retrotransposon
CR1A	178	192	223	329	334	207	8.83E-02	1.47	Retrotransposon
Diver	58	39	55	43	42	62	9.25E-01	0.96	Retrotransposon
DIVER2	18	32	26	30	26	20	9.54E-01	1.03	Retrotransposon
DM_ROO	510	1014	1140	1350	1226	769	5.00E-01	1.26	Retrotransposon
DM88	38	54	43	44	42	20	5.81E-01	0.80	Retrotransposon
DMGYPF1A	166	141	165	274	300	277	4.80E-04	1.80	Retrotransposon
DOC	2636	1966	2108	3450	3628	2834	4.25E-02	1.48	Retrotransposon
DOC2	225	167	177	211	185	176	9.81E-01	1.00	Retrotransposon
DOC3	231	276	326	462	457	333	4.49E-02	1.51	Retrotransposon

DOC4	14	26	24	30	87	30	5.48E-02	2.32	Retrotransposon
DOC5	11	26	35	33	25	17	8.96E-01	1.08	Retrotransposon
F-element	385	382	421	529	446	361	5.95E-01	1.13	Retrotransposon
Flea	733	737	825	1431	1294	783	6.13E-02	1.53	Retrotransposon
FROGGER	25	63	49	49	16	17	3.25E-01	0.61	Retrotransposon
FW2	18	31	29	23	23	10	5.36E-01	0.74	Retrotransposon
FW3	15	30	30	21	13	10	2.82E-01	0.60	Retrotransposon
G2	58	39	49	61	71	56	4.40E-01	1.28	Retrotransposon
G3	13	17	28	12	7	9	1.69E-01	0.51	Retrotransposon
G4	71	145	124	126	74	76	5.83E-01	0.82	Retrotransposon
G5	98	73	93	97	88	101	8.04E-01	1.08	Retrotransposon
G5A	138	158	182	169	135	126	7.02E-01	0.90	Retrotransposon
G6	24	21	31	37	59	57	2.96E-02	2.02	Retrotransposon
Gate	166	121	166	362	484	472	1.00E-08	2.90	Retrotransposon
GTWIN	14	12	16	20	39	16	2.10E-01	1.78	Retrotransposon
GYPSY10	90	135	101	118	84	83	6.83E-01	0.88	Retrotransposon
GYPSY11	10	7	24	12	11	10	1.00E+00	0.81	Retrotransposon
GYPSY2	29	29	21	36	37	42	2.88E-01	1.46	Retrotransposon
GYPSY4	41	50	56	67	82	49	3.59E-01	1.35	Retrotransposon
GYPSY5	4	6	11	16	15	8	1.00E+00	1.85	Retrotransposon
GYPSY6	12	20	25	27	26	17	6.08E-01	1.28	Retrotransposon
GYPSY8	38	25	28	12	25	31	5.43E-01	0.75	Retrotransposon
GYPSY9	37	32	54	42	13	13	2.27E-01	0.56	Retrotransposon
HeT-A	1033	1077	1180	1182	1283	798	9.78E-01	0.99	Retrotransposon
I-element	224	201	197	418	372	208	5.26E-02	1.61	Retrotransposon
Idefix	72	136	193	243	352	127	1.08E-01	1.81	Retrotransposon
INVADER	46	57	42	35	34	29	2.34E-01	0.68	Retrotransposon
INVADER2	38	66	77	140	192	118	9.10E-04	2.50	Retrotransposon

INVADER3	150	176	185	241	336	196	7.21E-02	1.51	Retrotransposon
INVADER4	19	34	37	61	77	47	2.58E-02	2.07	Retrotransposon
IVK	53	55	45	125	225	224	1.00E-07	3.73	Retrotransposon
Jockey	848	596	653	831	1122	1106	6.34E-02	1.46	Retrotransposon
Jockey_1	579	539	644	519	542	409	3.68E-01	0.83	Retrotransposon
JOCKEY2	99	152	146	98	83	47	5.90E-02	0.58	Retrotransposon
JUAN	80	96	97	165	265	133	4.37E-03	2.07	Retrotransposon
Max-element	859	779	364	1190	807	781	3.00E-01	1.39	Retrotransposon
MDG3	712	708	553	925	753	408	8.72E-01	1.06	Retrotransposon
MGD1	178	350	425	553	833	473	1.94E-02	1.95	Retrotransposon
Micrococpia	35	36	43	44	45	21	9.68E-01	0.98	Retrotransposon
ninja	33	28	39	17	33	23	4.44E-01	0.73	Retrotransposon
OPUS	1450	1511	1833	2025	2093	2767	6.66E-02	1.44	Retrotransposon
QBERT	17	30	31	36	42	47	1.74E-01	1.63	Retrotransposon
QUASIMODO	40	66	63	91	100	42	3.90E-01	1.39	Retrotransposon
R1-2	19	14	18	15	3	7	1.91E-01	0.50	Retrotransposon
R1A1-element	44	28	30	48	48	55	2.53E-01	1.46	Retrotransposon
ROOA_LTR	56	60	88	209	276	150	1.00E-05	3.13	Retrotransposon
ROVER	55	110	156	146	200	71	5.52E-01	1.30	Retrotransposon
Rt1a	27	41	32	55	54	30	3.64E-01	1.41	Retrotransposon
RT1B	136	171	167	183	212	143	6.19E-01	1.14	Retrotransposon
RT1C	26	19	25	19	19	20	6.90E-01	0.83	Retrotransposon
S-element	89	150	124	163	202	100	4.42E-01	1.28	Retrotransposon
S2	17	20	31	26	51	15	5.35E-01	1.38	Retrotransposon
SPRINGER	1363	1611	1080	2201	1600	1522	2.48E-01	1.31	Retrotransposon
STALKER2	55	145	139	115	112	79	8.19E-01	0.91	Retrotransposon
TABOR	41	126	162	131	106	54	8.24E-01	0.89	Retrotransposon
TARTC	56	45	72	107	183	94	5.13E-03	2.22	Retrotransposon

TOM1_LTR	28	52	76	66	105	69	2.58E-01	1.53	Retrotransposon
Transpac	458	1106	1447	2514	2842	820	2.94E-01	2.05	Retrotransposon
X-ELEMENT	68	45	55	62	53	55	9.78E-01	1.01	Retrotransposon
ZAM	29	35	37	27	21	27	4.38E-01	0.74	Retrotransposon
1360	416	775	710	1240	1224	734	4.76E-02	1.68	DNA
BARI1	27	46	40	70	67	48	1.12E-01	1.65	DNA
Hobo	90	185	138	175	188	155	4.45E-01	1.26	DNA
Pogo	216	500	487	612	774	365	2.69E-01	1.46	DNA
HB	78	148	151	178	200	157	2.08E-01	1.42	DNA
FB	98	177	215	152	259	105	9.03E-01	1.06	DNA
Hopper	9	37	20	30	41	23	4.70E-01	1.45	DNA
INE1	88	126	133	168	173	109	3.43E-01	1.31	DNA
MARINER2	84	113	114	98	81	89	6.01E-01	0.86	DNA
P-element	339	561	593	739	775	618	1.21E-01	1.43	DNA
TC1	89	112	75	144	171	58	4.30E-01	1.35	DNA
TC1-2	84	111	115	141	166	101	3.10E-01	1.32	DNA
TRANSIB2	35	86	70	61	52	23	4.49E-01	0.71	DNA
TRANSIB3	37	102	77	168	194	92	2.99E-02	2.12	DNA
TRANSIB4	14	14	12	23	17	9	7.19E-01	1.22	DNA

1030